https://doi.org/10.5194/essd-2020-47
Preprint. Discussion started: 7 April 2020


Open Access Earth System Science Data Discussions

# Greenland liquid water runoff from 1979 through 2017

Kenneth D. Mankoff[1], Andreas P. Ahlstrøm[1], William Colgan[1], Robert S. Fausto[1], Xavier Fettweis[2], Ken Kondo[3], Kirsty Langley[4], Brice Noël[5], Shin Sugiyama[3], and Dirk van As[1]

[1]Department of Glaciology and Climate, Geological Survey of Denmark and Greenland (GEUS), Copenhagen, Denmark
[2]Department of Geography, University of Liège, Belgium
[3]Institute of Low Temperature Science, Hokkaido University, Japan
[4]Asiaq-Greenland Survey, Nuuk, Greenland
[5]Institute for Marine and Atmospheric Research, Utrecht University, The Netherlands

**Correspondence:** Ken Mankoff (kdm@geus.dk)

**Abstract.** We provide high-resolution datasets of Greenland hydrologic outlets, basins, and streams, and a 1979 through 2017 time series of Greenland liquid water runoff for each outlet. Outlets, basins, and streams are derived from traditional hydrologic routing algorithms over the surface of a 100 m ArcticDEM digital elevation model (DEM) twice: Once to the ice margin and once to the coast. We then partition liquid water runoff from both ice and land from two regional climate models (RCMs; MAR and RACMO) into each basin and at each outlet location. The data include `18903` ice basins and outlets (`614` basins greater than 10 km$^2$), `30241` land basins and outlets (`958` basins greater than 10 km$^2$), major streams in each basin, and daily runoff water volume flow rate at each outlet from each of two RCMs. We perform a sensitivity study of outlet location change for every ice sheet location over a range of hydrologic routing assumptions and data sets. Annual runoff from the ice ranges from ~136 km$^3$ in 1992 to ~785 km$^3$ in 2012. Daily maximum ice runoff from one basin is as large as 4380 m$^3$ s$^{-1}$. Both ice runoff magnitude and variability increase over the time series. Land runoff contributes an additional ~35 % to the ice runoff. Comparison with 9 basins instrumented with stream gauges shows a range of (dis)agreement from poor to excellent between our estimated discharge and observations. As part of the journal's living archive option, and our goal to make an operational product, all input data, code, and results from this study will be updated as needed (when new input data are available, as new features are added, or to fix bugs) and made available at doi:10.22008/promice/data/freshwater_runoff/v01 (Mankoff, 2020) and at http://github.com/mankoff/freshwater.

## 1 Introduction

Over the past decades, liquid runoff from Greenland has increased (Mernild and Liston, 2012; Bamber et al., 2018; Trusel et al., 2018; Perner et al., 2019). When that runoff leaves the ice sheet and enters fjords and coastal seas, it influences a wide range of physical (Straneo et al., 2011; An et al., 2012; Mortensen et al., 2013; Bendtsen et al., 2015; Cowton et al., 2015; Mankoff et al., 2016; Fried et al., 2019; Cowton et al., 2019; Beckmann et al., 2019), chemical (Kanna et al., 2018; Balmonte et al., 2019), and biological (Kamenos et al., 2012; Kanna et al., 2018; Balmonte et al., 2019) systems (Catania et al., 2019). The scale of impacts ranges from the ice-ocean boundary to the distal open ocean (Gillard et al., 2016). The influence of freshwater on multiple domains and disciplines (Catania et al., 2019) is the reason several past studies have estimated runoff at various

https://doi.org/10.5194/essd-2020-47
Preprint. Discussion started: 7 April 2020


Open Access Earth System Science Data Discussions

temporal and spatial scales (Mernild et al., 2008, 2009, 2010; Langen et al., 2015; Ahlstrøm et al., 2017; Citterio et al., 2017; van As et al., 2018; Bamber et al., 2018; Perner et al., 2019; Slater et al., 2019).

Freshwater discharge from Greenland primarily takes three forms: solid ice from calving at marine terminating glaciers, submarine meltwater at marine terminating glaciers, and liquid runoff from surface melt, condensation, and rainfall. Immediately upstream from the grounding line, no submarine melting has occurred and that water is still solid ice. A recent paper by Mankoff et al. (2019) targets the solid ice discharge budget by estimating solid ice discharge across flux gates 5 km upstream from all fast-flowing marine terminating glaciers in Greenland. Complementing that paper, this paper targets Greenland's point-source liquid water runoff budget by partitioning RCM runoff estimates to all ice margin and coastal outlets. The sum of this data product and Mankoff et al. (2019) is an estimate of the majority of freshwater (liquid and solid ice) volume flow rates into Greenland fjords. Those two terms comprise the bulk but not all of freshwater volume - they exclude relatively minor contributions from precipitation directly onto the fjord surface, evaporation and condensation, sea ice formation and melt, or subglacial basal melting. Much work remains to determine which portion of solid ice across a flux gate becomes submarine melt, and where and when the solid ice, i.e. icebergs, melts in the fjord.

In this data set description we present a Greenland wide product of liquid water runoff time series and a high-resolution map of hydrologic outlets, basins, and streams. The daily runoff water volume flow rate for the period of 1979 through 2017 are based on runoff from land or ice estimated by two regional climate models (RCMs) and has a 100 m spatial resolution including outlets, basins, and streams (at the ice margin and coast). In the following description and methods, we document the inputs, assumptions, methodologies, and results we use to estimate Greenland runoff from 1979 through 2017. This product is available at doi:10.22008/promice/data/freshwater_runoff/v01 (Mankoff, 2020).

## 2 Input Data

The static products (streams, outlets, and basins (Fig. 1)) are derived from an ice-sheet surface DEM, an ice-sheet mask, the land surface DEM, and an ocean mask. For the surface DEM, we use the ArcticDEM v7 100 m product (Porter et al., 2018). When using subglacial routing, we use ice thickness from BedMachine v3 (Morlighem et al., 2017b, a). For the ice mask we use the Programme for Monitoring of the Greenland Ice Sheet (PROMICE) Ice Extent (Citterio and Ahlstrøm, 2013). For the ocean mask we use the Making Earth System Data Records for Use in Research Environments (MEaSUREs) Greenland Ice Mapping Project (GIMP) Land Ice and Ocean Classification Mask, Version 1 (Howat, 2017b; Howat et al., 2014). Satellite basemap imagery comes from (Howat et al., 2014), specifically the National Snow and Ice Data Center (NSIDC) MEaSUREs GIMP data set with ID 0713 (Howat, 2017a).

The time series product (daily runoff) is derived from gridded daily runoff estimates from RCM calculations over the land and ice areas of Greenland. The daily runoff comes from the Modèle Atmosphérique Régional (MAR; Fettweis et al. (2017),

https://doi.org/10.5194/essd-2020-47
Preprint. Discussion started: 7 April 2020


Open Access Earth System Science Data Discussions

15 km resolution) and the Regional Atmospheric Climate Model (RACMO; Noël et al. (2019), 5.5 km resolution) and runoff, $R$, is defined by

$$R = ME + RA - RT - RF \tag{1}$$

where $ME$ is melt, $RA$ is rainfall, $RT$ is retention, and $RF$ is refreezing. In RACMO, retention occurs only when there is firn, not with bare ice, while MAR has a runoff delay for bare ice runoff, but not land runoff. Both RCM results were provided regridded to a 1 km resolution using an offline statistical down-scaling technique based on local vertical runoff gradient applied to the sub-grid topography. MAR simulations were run using version 3.9.6 (Delhasse et al., 2019). RACMO simulations were run using version 2.3p2 (Noël et al., 2018). Both RCMs use ERA-Interim 6-hour forcing.

## 3 Methods

Streams are calculated from the hydrologic head elevation, that is the DEM surface for surface routing, or the subglacial pressure head elevation for subglacial routing (only performed as part of the uncertainty estimate). Outlets are defined as the grid cell location where streams terminate at the ice margin or coastal boundary. Each outlet has one upstream basin and each basin has one outlet. Only major streams are defined, so small basins may have outlets but no streams.

We use the GRASS GIS software package (Neteler et al., 2012; GRASS Development Team, 2018) `r.stream.extract` tool configured for multi-flow direction from eight neighbors (MFD-8) to calculate the primary flow direction and outlets at the ice edge and coast, and then the `r.stream.basins` tool to calculate basins and streams upstream from each outlet (Jasiewicz and Metz, 2011). Basins < 1 km$^2$ are absorbed into their largest neighbor and the associated outlets are dropped.

Finally, for both domains (land and ice) we calculate zonal statistics for each basin and day for the RCM ice and land runoff. Outlet metadata data includes the BedMachine elevation at the outlet location. When this value is negative, it indicates submarine (subglacial) discharge.

### 3.1 Coverage

Each 100 m$^2$ pixel is classified as ice, land, or fjord. However, the ice boundary (Citterio and Ahlstrøm, 2013), the coast boundary (Howat, 2017b), and the 1 km$^2$ statistically-downscaled RCM domains do not always agree with each other on the classification of a given grid cell. A disagreement occurs, for example, when a basin cell is classified as glacier in Citterio and Ahlstrøm (2013) but the matching RCM cell is land, or vice versa. This disagreement occurs almost everywhere along the ice margin because the 1 km resolution RCM boundary and the 100 m mask boundary rarely perfectly align. It also occurs wherever nunatuks exist, because ice-sheet interior "holes" are filled, otherwise they falsely act as interior drains. The ice margin is also where the majority of runoff occurs due to the highest temperatures at the lowest ice elevations. Small changes in masks in these locations can introduce large changes in RCM outputs.

https://doi.org/10.5194/essd-2020-47
Preprint. Discussion started: 7 April 2020


Open Access Earth System Science Data Discussions

We adjust the RCM results to the basin using the following method (Fig. 2). Where the surface mask reports ice and a RCM reports land, the RCM land runoff fraction is discarded (this reduces annual average runoff by ~5 %), and the RCM ice runoff fraction over this basin is used to compensate for the uncovered basin cells. For example, if an ice basin is only 90 % covered by ice in an RCM, the runoff is divided by 0.9 to estimate total runoff. Where a basin reports land and the RCM reports ice, the same method as above is applied, but for land. When a small basin has no RCM cells of the same classification covering any part of it, that basin never has any reported runoff. This method means that RCM runoff is not conserved through this work - RCM inputs to our algorithm do not equal our reported output which are ~3 % higher on an annual average.

Runoff adjustments using this method are underestimated for large basins with large inland high elevation regions with low runoff, because this method fills in misaligned cells with each days average runoff, but the misalignment (missing runoff) occurs at the ice sheet edge where maximum runoff occurs. However, given that the basin is large, misalignment is proportionally small, and therefore errors are proportionally small. When misalignment is proportionally large (e.g. a basin is only ~1 % covered by the same RCM classification), that implies a small basin. In the case of a small basin, the covered part must be near the uncovered part, the infilling method therefore uses spatially nearby data, and there is no underestimate.

At the basin scale, fractional coverage ranges from 0 to 1. Coverage equal to 0 occurs where a basin does not have a MAR or RACMO cell of the same type (ice or land) over any part of it. Coverage close to 0 occurs where a basin has one grid cell (100 $m^2$) overlapped by a MAR or RACMO cell of the same type, but the rest of the basin has no overlap. Coverage equal to 1 occurs where a basin is completely overlapped by MAR or RACMO cells of the same type.

RCM inputs are also scaled by the projection area error between the EPSG:3413 map projection of the RCM and an approximation of the true earth spheroid. This error is up to 8 % for some grid cells, but ranges from - 6 % to + 8 % over Greenland and the cumulative error for the entire ice sheet is < 8 %.

## 4 Product Description

This liquid water runoff product for Greenland contains a static map of Greenland's hydrological outlets, basins, and streams and a times-series of runoff from each outlet.

The output data is provided in the following formats: The stream product is provided as a GeoPackage standard GIS product and a metadata CSV that includes the stream type (start or intermediate segment), network, stream along-flow length, stream straight length, sinuosity, source elevation, outlet elevation, and a variety of stream indices such as the Strahler, Horton, Shreve, Hack, and other parameters (Jasiewicz and Metz, 2011). The outlet product is also provided as a GeoPackage and CSV, each of which include the outlet ID (linked to the basin ID), the longitude, latitude, EPSG:3413 x and y, and the outlet elevation. The basin product GeoPackage includes the geospatial region that defines the basin. The metadata CSV includes the basin ID (linked to the outlet ID), and the area of each basin. The time-series discharge product is provided as annual NetCDF files, four per year, one for each domain (ice margin, land coast) and one for each RCM (MAR and RACMO). The NetCDF file contains an unlimited time dimension, usually containing 365 or 366 days, much of the same metadata as the outlets CSV file, including

https://doi.org/10.5194/essd-2020-47
Preprint. Discussion started: 7 April 2020


Open Access Earth System Science Data Discussions

the outlet (a.k.a station) ID, the latitude, longitude, and altitude of the outlet, and a runoff variable with dimensions (station, time) and units $m^3\ s^{-1}$.

## 5 Results

Results of this work include 1) ice-margin terminating streams, outlets, and basins, 2) coast-terminating streams, outlets, and basins (this product is a super-set of (1), and includes the upstream ice streams and basins), 3) runoff at the ice-marginal outlets from ice runoff and 4) runoff at the coastal outlets from land runoff. Runoff ice products are in duplicate from the MAR and RACMO RCMs.

Fig. 1 illustrates `18903` ice basins and outlets and `30241` land basins and outlets. Among these ice basins we find `614` greater than 10 $km^2$ and `42` greater than 100 $km^2$, while the land basins have `958` greater than 10 $km^2$ and `47` greater than 100 $km^2$.

Overall this amounts to 1,807,264 $km^2$ of basin ice cells, of which 1,769,087 $km^2$ are covered by ice in MAR, 37,669 $km^2$ are covered by land, and 479 $km^2$ are covered by fjord. There are 336,497 $km^2$ of basin land cells, of which 306,256 $km^2$ are covered by land in MAR, 10,569 $km^2$ are covered by ice, and 19,672 $km^2$ are covered by fjord. The total Greenland coverage of RACMO is similar (Table and data available in Supplemental Online Material).

Our grid cell land classification correction adjusts RCM ice runoff values by ~8 %. As mentioned, the misalignment between the ice, land, and ocean masks and the RCM land type results in a total ice sheet runoff ~5 % less than the RCM runoff inputs when runoff is only accumulated where the RCM ice grid cells align with the basin ice grid cells. However, when our coverage algorithm is subsequently applied to adjust RCM inputs for regions where basins have ice but the RCMs do not, total ice sheet runoff is ~3 % more than the RCM inputs. A similar adjustment occurs for RCM land runoff.

Figure 3 shows the time-series product spanning the period from `1979` through `2017`, containing `14244` days. Daily runoff values range from a minimum of 0 $m^3$ to a maximum of `4380` $m^{-3}$ on `'2012-08-06'` located on the western part of the ice sheet south of Sermeq Kujalleq (Jakobshavn Isbræ) (50.68 E, 68.31 N, 203 m a.s.l). Annual runoff has a maximum of `18` $km^3$ from one basin (a similar value as reported by Lewis and Smith (2009)).

Annual average ice runoff has a 1979 through 2017 mean of ~400 ±30 $km^3$ (± 15 %), a 1992 minimum of 136 ± 10 $km^3$ (MAR ice) and 191 ± 14 $km^3$ (RACMO ice), and a 2012 maximum of 785 ± 59 $km^3$ (MAR) and 693 ± 50 $km^3$ (RACMO) (Fig. 3). The 1992 low is likely due to the Mt. Pinatubo eruption, and then 2nd lowest runoff year, 1983, due to El Chichón eruption. The land runoff (MAR only) contributes an additional 35 % to the ice runoff on average, with a range from 18 % (142 ± 10 $km^3$ during the 2012 high ice-runoff year) to 83 % (112 ± 8 $km^3$ during the 1992 low ice-runoff year).

During the first decade of the time series, ice runoff had a mean of 305 ± 23 $km^3$ (MAR) or 325 ± 24 $km^3$ (RACMO), ranged from ~200 ± 15 $km^3$ to ~390 ± 30 $km^3$, and had an annual standard deviation of 60 $km^3$. During the last decade of the time series, ice runoff had a mean of 531 ± 38 $km^3$ (MAR) or 519 ± 38 $km^3$ (RACMO), ranged from ~370 ± 28 $km^3$ to 785 ± 59 $km^3$, and had an annual standard deviation of 130 $km^3$. From this, it is evident that ice runoff varies widely but increases in both magnitude and variability over the duration of the time-series.

https://doi.org/10.5194/essd-2020-47
Preprint. Discussion started: 7 April 2020



## 6 Discussion

### 6.1 Comparison with previous similar work

Our static products - streams, outlets, and basins - have been previously estimated. Lewis and Smith (2009) identified 293 distinct hydrologic ice basins and provided a data set of ice basins and ice margin outlets. Our work, a decade later, has significantly more basins and outlets because of the higher resolution of the input data, and additional data products. We provide ice basins, ice margin outlets, ice streams with metadata, land basins, coastal outlets, and land streams with metadata. Lewis and Smith (2009) generated basins from a 5 km DEM, compared to the 100 m DEM used here. Routing with a 5 km DEM is likely to cause some basins and outlets to drain into an incorrect fjord. When comparing BedMachine v3 (150 m) and ArcticDEM (100 m) products, land DEM errors or resolution limitations cause some BedMachine basins to drain on the opposite side of a spit or an isthmus than they appear to in satellite imagery - imagery that is closely matched by the nearby flow-path as routed using ArcticDEM.

Our time-series product - runoff, also has existing similar products. The most recent of these is from Bamber et al. (2018) (Fig. 3) who provide a data product at lower spatial resolution (5 km), lower temporal resolution (monthly), and only coastal discharge, not coastal basins, nor ice basins, nor ice margin outlets and discharge. However, Bamber et al. (2018) surpasses our product in that the time-series extends back to 1958, and spatial coverage includes a larger portion of the Arctic including Iceland, Svalbard, and Arctic Canada. Furthemore, by providing data at 5 km spatial and monthly temporal resolution, Bamber et al. (2018) implements the main strategy suggested here to increase the signal-to-noise ratio of the data.

### 6.2 Validation against observations

There are many regional products that estimate a single or a few basins and associated runoff over a range of spatial resolutions and a range of temporal resolutions and periods. Examples of these include Rennermalm et al. (2012); Lindbäck et al. (2014, 2015); Ahlstrøm et al. (2017); van As et al. (2017, 2018) and others. Many of these regional studies focus on the oft-studied south-west sector of Greenland that includes the Russell and Leverett glaciers and the Watson River. Here we compare our results to all observations that we have been able to find that are publicly accessible, or willing to become open and publicly accessible as part of this work. These comparisons include (1) Watson River discharge from van As et al. (2018), (2) Greenland Ecosystem Monitoring Programme (GEM) data for six basins around Zackenberg, Disko Island, and Nuuk, and (3) Runoff from a small basin near Qaanaaq, in Northwest Greenland.

#### 6.2.1 Watson River

We compare the observed Watson River discharge from van As et al. (2018) to the runoff from the nearest outlet in this work. We note that runoff from this work matches for low runoff ($< 500$ m$^3$ s$^{-1}$, 93 % of all runoff days), but is only approximately half of the van As et al. (2018) runoff for high runoff (Fig. 4). This difference may be due to either errors in the basin delineation used in this study, errors in the stage-discharge relationship used by van As et al. (2018), errors in the RCM runoff estimates, or

https://doi.org/10.5194/essd-2020-47
Preprint. Discussion started: 7 April 2020


a combination of the above three. All three of these error sources increase with high melt or runoff; Basin delineation becomes less certain with distance from the ice sheet margin. The river stage-discharge conversion becomes less certain at high stage levels. Runoff calculations from a snow surface are more uncertain than from an ice surface, because of e.g. snow density, subsurface refreezing, and surface darkening.

Our basin is smaller than the basin used in van As et al. (2018) and similar to Mernild et al. (2018) who attributed the difference between their modeled outflow and observations from van As et al. (2017) to their decision to use surface rather than subglacial routing, and applied a correction term. We find that our basin does not include ice to the south of itself that is included in van As et al. (2018). When we manually add the two large ice basins to the south of the Watson River basin, runoff estimates agree (Fig. 4 right panel), suggesting basin delineation, not stage-discharge or RCM may be the primary cause for this disagreement. We are able to recreate the van As et al. (2018) basin (introduced in Lindbäck et al. (2015)) but only when using the Lindbäck et al. (2014) bed and the Bamber et al. (2013) surface. When using only one or zero of those and any combination of BedMachine v2 (Morlighem et al., 2014), BedMachine v3, or ArcticDEM surface elevations and BedMachine v2 or v3 bed elevations, we are unable to match the Lindbäck et al. (2015) basin. Instead all our basins resemble those shown in Fig 5.

#### 6.2.2 GEM Basin Outlets

Six basins from the GEM project have a time-series of runoff (Langley, 2020), and comparisons between our basin-partitioned RCM runoff and observations show better agreement than for the Watson River basin(s). We note that these basins are significantly smaller than the Watson River basin, but because the basin is primarily defined by a land surface rather than an ice basin, basin delineation is more accurate. Therefore disagreement here between GEM observation and our product is likely attributable to errors in the RCM runoff, not the basin delineation.

Of the six basins with GEM runoff, the two largest (Zackenberg (Fig. 7) and Røde Elv (Fig. 8)) show most ice basins are overlapped by MAR and RACMO ice cells, although two ice basins are not covered by RCM ice cells in the Zackenberg basin, and a without an ice basin does have RCM ice cells in the Røde Elv basin. The four smallest GEM basins (Fig. 9) have only one MAR and RACMO ice cell over an ice basin, several ice basins with no simulated runoff, and several MAR and RACMO ice cells with no co-located ice basin. The discussion of how these (mis)alignments are treated is in Sec. 3.1.

We show both daily time-series (Fig. 10) and 10-day smoothed scatter-plot (Fig. 11) of the six GEM basin runoff observations and estimates. We use only MAR as the comparison here because the MAR product includes land and ice runoff, while RACMO only includes ice runoff. The daily time series, limited to 2017 because that is the only year of Røde Elv data, shows an agreement in both magnitude and variability between the MAR and GEM runoff products. However, all basins except Zackenberg show a MAR step-change decrease between day 168 and 169, after which variability continues to match (e.g. modeled vs. observed day-long precipitation events roughly align) but magnitude does not agree as well as prior to day 169.

The scatter plot has a 10-day smooth applied as in van As et al. (2017), and shows all available days of data not just 2017. Color represents day of year, and similar to Fig. 10 shows that the MAR runoff slightly overestimates the GEM observations early in the year, and slightly underestimates the observations late in the year.

https://doi.org/10.5194/essd-2020-47
Preprint. Discussion started: 7 April 2020


This seasonal disagreement is apparent as a step-change in all years, but not always on day 169 (18 June for non-leap-years). However, sometime in June of all years where GEM data and MAR data exist and in five of six basins (excluding Zackenberg), a step-decrease in MAR produces an underestimate of runoff relative to observations. The cause for this disagreement is not yet known.

#### 6.2.3 Qaanaaq Glacier Outlet

We validate our basins and runoff against one additional observation and highlight that in some locations strong agreement exists but may or may not exist for the right or wrong reason. A small basin near Qaanaaq has been instrumented for the past several summers (Sugiyama et al., 2014; Tsutaki et al., 2017; Kondo and Sugiyama, 2020), with overlap in August 2017.

From Fig. 12, the Qaanaaq glacier outline is closely matched by the ice basin product generated here. However, only one nearby MAR ice cell covers 4 of the 1075 basin grid cells. Even so, that single MAR cell combined with our coverage algorithm (Sec. 3.1) generates very good agreement between MAR runoff and observations (Fig. 13). MAR runoff relative to observations ranges from 20 % under (last day of time series) to 140 % over (28 July). When excluding 27 and 28 July where MAR runoff increases prior to observations, maximum overestimate is 50 % on 31 July. The total summed difference between MAR and observations over the course of this time-series is 12 %.

RACMO ice cells cover almost the entire ice basin, yet RACMO runoff does not agree as well with observations as MAR runoff. The comparison here is among observations from a stream, MAR ice and land, and RACMO ice only. Land area is not included in the RACMO product, but excluding it here is not likely to be the reason for the disagreement given a) the relatively small portion of the catchment that is land and b) the magnitude of the MAR-estimated land runoff. Regardless, here RACMO does not capture the 5-fold increase seen in both the MAR and observations. The total summed difference between RACMO and observations over the course of this time-series is 43 %. This (dis)agreement among MAR, RACMO, and the observations highlights the uncertainty in the results presented here.

#### 6.2.4 Leverett Glacier Outlet

Leverett glacier runoff from 2009 through 2012 (Figs. 14 and 15) show a range of agreements and disagreements relative to observations (Tedstone et al., 2017; Hawkings et al., 2015). In 2009 and 2010, early season magnitude and variability matches (MAR better than RACMO), but there is more runoff in the models than the observations in July and August when large runoff occurs. All of 2011 is overestimated by the model, except a late August melt spike showing good agreement, albeit a slight lag between the model signals and the observations. The high runoff 2012 year shows better agreement between models and observations than the previous three years. In all cases, RACMO has significantly higher variability than MAR and the observations.

https://doi.org/10.5194/essd-2020-47
Preprint. Discussion started: 7 April 2020


#### 6.2.5 Other Proxy Observations

We are unaware of any additional stream gauge observations with open data that support comparison. However, a range of indirect and proxy observations exist, such as Mankoff et al. (2016) and Stevens et al. (2016) who find good agreement between runoff estimates using the same basin delineation theory as used here, observations of fjord salinity, and a plume model driving submarine glacier terminus melt.

### 6.3 Uncertainty

Uncertainty from RCM inputs and observations are considered external to this work, although they are still discussed below. In this work, we introduce one new source uncertainty - the routing model, which exhibits in two different ways: Spatial (basin delineation) and temporal (runoff delay).

We do not address the temporal uncertainty quantitatively or numerically in this work - only in discussion throughout the document and in the Mitigation section. Spatial uncertainty is a product of both the input data (the BedMachine bed) and the subglacial routing assumptions (the $k$ value in Equation 2). Estimating these uncertainties may or may not lead to different estimates of runoff - for example, two drastically different drainage basins from different $k$-values may have similar estimates of runoff. The inverse is less common - it is not likely to have drastically different outlet runoff estimates from basins with only small changes, because large volumes of runoff usually come from large areas.

#### 6.3.1 Basin uncertainty and surface vs. subglacial routing

The basins presented here are static approximations based on 100 m resolution surface DEM of a dynamic system. It is difficult to quantify the uncertainty of the assumptions used here, but we discuss the known uncertainties, ranging from least uncertain to most uncertain.

Basins comprised of only land are likely to be more precise and accurate than ice basins, because land is better resolved, has larger surface slopes, has negligible sub-surface flow, and is less dynamic than ice. Even if basins and outlets seem visually correct from the 100 m product, the basin outline still has uncertainty on the order of hundreds of meters and will therefore include many minor errors and non-physical properties, such as drainage basin boundaries bisecting lakes.

Basins delineated using the ice surface are likely to be more precise than basins using static subglacial theory, because the ice surface elevation has smaller errors than the bed elevation. However, even if more precise, they may be less accurate, because most water routes subglacially. Finally, the precision and accuracy differences increase when one considers that subglacial routing is highly dynamic on timescales from minutes to seasons (e.g. Werder et al. (2013)). This dynamic system may introduce large spatial changes in outflow location (water or basin "piracy", Ahlstrøm et al. (2002); Lindbäck et al. (2015); Chu et al. (2016)), but recent work by Stevens et al. (2018) suggests basins switching outlet locations may not be as common as earlier work suggests, and our sensitivity analysis (Fig. 6 and Appendix) suggests that for source locations where the majority of runoff occurs, outlet location change by less than 10 km under different routing assumptions and data sets. Subglacial routing also increases opportunities for subglacial storage (Rennermalm et al., 2013; Livingston et al., 2013).

https://doi.org/10.5194/essd-2020-47
Preprint. Discussion started: 7 April 2020


We note that the ice surface is responsible for ~90 % of the subglacial routing assuming equal gradients at the ice surface and base. If basal features are ~10x the size of surface features, then the ice surface is effectively responsible for ~50 % of subglacial routing.

Finally, subglacial routing introduces hydraulic jumps because the BedMachine bed and thickness products, the Citterio and Ahlstrøm (2013) ice and land mask, and the ArcticDEM ice surface are not all perfectly aligned.

Given all of the above considerations, we opted for surface routing rather than subglacial (similar to Ahlstrøm et al. (2017) and Mernild et al. (2018)). However, we compare surface and subglacial basins (even with hydraulic jumps), and the influence of those basins on the final outflow location, across a variety of products, where we quantify for every grid cell how far the eventual outlet for that grid cell moves under different basin delineation schemes.

When routing subglacially, we define the head $h$ as

$$h = z_b + k\frac{\rho_i}{\rho_w}(z_s - z_b), \tag{2}$$

where $h$ is the hydraulic head at each location, $z_b$ the ice-free land surface and basal topography, $k$ the flotation fraction, $\rho_i$ the density of ice (917 kg m$^{-3}$), $\rho_w$ the density of water (1000 kg m$^{-3}$), and $z_s$ the land surface for both ice free and ice covered surfaces. Equation 2 comes from Shreve (1972) where they define the hydropotential (units Pa), but here is divided by gravity $g$ times the density of water $\rho_w$ to convert the units from units Pa to m. Equation 2 makes the assumption that when ice is present ($z_s \neq z_b$) all water routes subglacially. When $k$ is equal to $\rho_w/\rho_i \approx 1.0905$, then Eq. 2 simplifies to $h = z_s$.

Fig. 6, comparing ArcticDEM surface routing vs. BedMachine surface routing, shows that part of one basin shifts its coastal outlet by 30 to < 100 km, a few smaller portions of basins shift their outlets by 10 to < 30 km, Sermeq Kujalleq (Jakobshavn Isbræ) by 3 to < 10 km, and the majority by < 1 km. A range of additional routing scheme and input data set comparisons are shown in the Appendix.

Finally, even when we perform surface routing for basin delineation, we provide the BedMachine elevation of each outlet. Outlet elevations less than 0 indicate marine terminating subglacial outlets. However, even though this method provides an estimate of the initial subglacial discharge depth, much work remains to determine the effective depth of subglacial discharge, where effective depth is defined as the neutrally buoyant isopycnal that the subglacial discharge rapidly reaches once it enters the fjord (c.f. Mankoff et al. (2016)).

#### 6.3.2 RCM uncertainty

In addition to the basin delineation issues discussed above, the runoff product from the RCMs also introduces uncertainty into the product generated here. The RCM input products do not provide formal time- or space-varying error estimates, but of course do contain errors because they do not precisely nor accurately capture reality. RCM uncertainty is assigned a fixed value of 15 %.

https://doi.org/10.5194/essd-2020-47
Preprint. Discussion started: 7 April 2020


The primary RCM issues include 1) general calibration error, 2) treatment of the time delay for runoff, and 3) low resolution in the spatial grid (sub-grid processes are not captured sufficiently and are often parameterized to agree with limited available observations e.g. density of fresh snow).

The first issue is highlighted above where we compare our runoff to observations, and see for example annually repeating step-changes in RCM runoff that do not match observations.

For the second issue, the RCMs do calculate refreezing in snow and firn, and the RACMO runoff equation does include a retention term, but retention only occurs when there is firn cover. MAR includes a time delay of up to 10 days that is primarily a function of surface slope (Zuo and Oerlemans, 1996; Yang et al., 2019). Neither model includes the subglacial system and runoff is assumed to immediately leave the ice sheet surface. Properly addressing time delays with runoff requires addressing storage and release of water across a variety of timescales in a variety of media: firn (e.g. Munneke et al. (2014); Vandecrux et al. (2019)), supraglacial streams and lakes (e.g. Zuo and Oerlemans (1996); Smith et al. (2015); Yang et al. (2019)), the subglacial system (e.g. Rennermalm et al. (2013)) and a variety of other physical processes that are not within the scope of SMB modeling. Runoff delay can be implemented outside the RCMs (e.g. Liston and Mernild (2012); Mernild et al. (2018)), but for this version of the product we present instantaneous runoff and downstream users can apply temporal lags if needed.

The third issue is a current limitation of the RCMs that will be improved as future versions increase resolution.

#### 6.3.3 Observational Uncertainty

When comparing against observations, additional uncertainty is introduced because the stage-discharge relationship is neither completely precise or accurate. We use published observation uncertainty when it exists.

#### 6.3.4 Mitigating Uncertainties

Traditional uncertainty propagation is further complicated because it is not clear to what extent the three uncertainties (observational, RCM, and routing model) should be treated as independent from each other - all three uncertainties are likely to show some correlation with elevation, slope, air temperature, or other shared physical processes.

Many of the uncertainties discussed here can be mitigated by increasing the signal to noise ratio of the product provided here. Because we provide a high spatial and temporal resolution product, this is equivalent to a large number of signals, each of which has some uncertainty (noise). Averaging results spatially or temporally, if possible for a downstream use of this product, will increase the signal to noise ratio and reduce uncertainty.

For example, because we provide basins for the entire ice sheet, total runoff is not subject to basin uncertainty. Any error in the delineation of one basin must necessarily be corrected by the inclusion (if underestimate) or exclusion (if overestimate) of a neighboring basin, although neighboring basins may introduce their own errors. Therefore, summing basins reduces the error introduced by basin outline uncertainty, and should be done if a downstream product does not need an estimate of runoff from a single outlet. This feature is built-in to coastal outlet discharge which is not as sensitive to our routing algorithm as ice margin outlet discharge because most coast outlets include a range of upstream ice margin outlets (e.g. Figs. B1 vs. B5 in Appendix).

https://doi.org/10.5194/essd-2020-47
Preprint. Discussion started: 7 April 2020


Conversely, at the ice margin, outlet location and discharge volume is more uncertain. However, most runoff is generated near the ice margin and as runoff approaches the margin, there is less opportunity for it to switch basins.

Temporally, errors introduced by this study's assumption of instantaneous runoff can be reduced by summing or averaging runoff over larger time periods. Although a given volume of water may remain in storage long term, the assumption of steady state storage means that long-term storage shown by, for example, dye trace studies, can be ignored - the volume with the dye may be stored, but a similar volume should be discharged in its place.

### 6.4 Other sources of freshwater

The liquid water runoff product provided here is only one source of freshwater that leaves the ice sheet and affects fjords and coastal seas. The other primary freshwater source is iceberg calving and submarine melt at the ice/ocean boundary of marine terminating glaciers. A companion to the liquid water runoff product introduced here is provided by Mankoff et al. (2019), which estimates solid ice volume flow rates across gates near marine terminating glaciers. That ice downstream enters fjords as either calving icebergs or liquid water from submarine melting.

Both this product and Mankoff et al. (2019) provide liquid or solid freshwater volume flow rates at outlets (this product, which includes elevation of discharge, equal to depth when negative) or grounding lines (Mankoff et al., 2019), but actual freshwater into a fjord occurs at a more complicated range of locations. Solid ice melts throughout the fjord and beyond (e.g. Enderlin et al. (2016); Moon et al. (2017)), and the freshwater discharge presented here may enter at a depth, but rapidly rises up the ice front and eventually flows into the fjord at some isopycnal (Mankoff et al., 2016). The eventual downstream location of the fresh water is not addressed in this work.

Freshwater inputs directly to the water surface are also not included in this product. The flux (per square meter) to the water surface should be similar to the flux to the non-ice-covered land surface - assuming the orographic effects on precipitation produce similar fluxes to the near-land water surface. The land runoff volume accounts for ~35 % of the total runoff volume presented in this work (Fig. 3), so the freshwater input (i.e. precipitation) directly to the fjord surface may be of similar magnitude.

Finally, basal melt from 1) geothermal heating (e.g. Fahnestock et al. (2001)) 2) frictional heating (e.g. Echelmeyer and Harrison (1990)) and 3) viscous heat dissipation from all previous freshwater sources (c.f. Mankoff and Tulaczyk (2017)) contributes up to 10 % additional runoff to the surface melt. Geothermal and frictional heating are approximately steady state and contribute freshwater throughout the winter months.

Importantly, ice sheet runoff may not be the majority source of freshwater into some fjords, even though it is traditionally considered the majority, or even only, source of freshwater. The combination of land runoff, freshwater inputs (snow and rain) directly onto the near-land fjord surface, and basal runoff, suggests that GIS-wide ice sheet surface runoff may account for < 50 % of total freshwater input. The percent contribution of ice sheet surface runoff to total freshwater input is likely to vary widely depending on the area considered for the downstream fjord, the upstream basin, and the dates and time-span of the estimates.

https://doi.org/10.5194/essd-2020-47
Preprint. Discussion started: 7 April 2020




## 7 Data and Code Availability

This work in its entirety is available at doi:10.22008/promice/data/freshwater_runoff/v01 (Mankoff, 2020) where it will be updated over time.

A website for post-publication updates is available at https://github.com/mankoff/freshwater where we document ongoing changes to this work and use the GitHub Issues feature to collect suggested improvements, document those improvements as they are implemented, document problems that made it through review, and mention related works not cited here, perhaps due to temporal directionality (Zeh, 2007). This version of the document is generated with git commit version 6fafea6 .

Runoff can only change in the future - the true past runoff is fixed - yet different estimates exist of past runoff (e.g. van As et al. (2018); Bamber et al. (2018), and this work). These differences must be caused by different methods or different inputs to the methods. By fully documenting the inputs, methods, and results we use to estimate runoff, this work supports attribution of result differences between different estimates. Both data and code are needed to support reproducibility, which is needed to both quantify and attribute differences. That is, future estimates of past runoff can and should both quantify and attribute differences due to changes in input data and the same methods (RCM inputs or the surface or subglacial digital elevation models (DEMs) used for routing), differences due to changes in hydrological routing algorithms using the same data, or combinations of the two. Quantification and attribution of these differences in needed to move the community from broadly comparable process studies to operational products that better support downstream research goals.

## 8 Conclusions

Our new outlet, basin, stream, and liquid water discharge data provide a high spatial (100 m) and temporal (1 day) resolution estimate of freshwater fluxes into Greenland fjords and coastal seas for the entire ice-sheet area from 1979 through 2017. We find an annual average Greenland runoff of 400 ± 30 $km^3$ ranging from 136 ± 10 $km^3$ in 1992 to 785 ± 59 $km^3$ in 2012, and displaying and overall increase in both magnitude and variability.

Because of the high spatial and temporal resolution, quality issues exist at basin and daily scale that do not exist when working over larger areas or times.

This liquid freshwater volumetric flow rate product is complemented by a solid ice discharge product (Mankoff et al., 2019). Combined, these provide an estimate of the majority of freshwater (total solid ice and liquid) flow rates from the Greenland ice sheet into fjords and coastal seas.

This estimate of freshwater flux into Greenland fjords aims to support further studies of the impact of freshwater on ocean physical, chemical, and biological properties; fjord nutrient, sediment, and ecosystems; and larger societal impacts of freshwater on the fjord and surrounding environments.

*Author contributions.*

https://doi.org/10.5194/essd-2020-47
Preprint. Discussion started: 7 April 2020




KDM produced this work - wrote the code and the text. APA and DVA helped with discussions of methods and quality control. WC, RSF, and DVA helped with writing. KK and SS supplied Qaanaaq data. XF and BN supplied RCM inputs. KL provided GEM data.

*Competing interests.*

The authors declare that they have no conflict of interest.

*Acknowledgements.* Funding was provided by the Programme for Monitoring of the Greenland Ice Sheet (PROMICE). Parts of this work were funded by the INTAROS project under the European Union's Horizon 2020 research and innovation program under grant agreement No. 727890. DEMs provided by the Polar Geospatial Center under NSF-OPP awards 1043681, 1559691, and 1542736. Data from the Greenland Ecosystem Monitoring Programme (GEM) were provided by Asiaq – Greenland Survey, Nuuk, Greenland. We thank Dorthe Petersen (ASIAQ) for help with basin quality control.

https://doi.org/10.5194/essd-2020-47
Preprint. Discussion started: 7 April 2020




## References

Ahlstrøm, A. P., Petersen, D., Langen, P. L., Citterio, M., and Box, J. E.: Abrupt shift in the observed runoff from the southwestern Greenland ice sheet, Science Advances, 3, e1701 169, https://doi.org/10.1126/sciadv.1701169, http://dx.doi.org/10.1126/sciadv.1701169, 2017.

Ahlstrøm, A. P., Bøggild, C. E., Mohr, J. J., Reeh, N., Christensen, E. L., Olesen, O. B., and Keller, K.: Mapping of a hydrological ice-sheet drainage basin on the West Greenland ice-sheet margin from ERS-1/-2 SAR interferometry, ice-radar measurement and modelling, Annals of Glaciology, 34, 309–314, https://doi.org/10.3189/172756402781817860, http://dx.doi.org/10.3189/172756402781817860, 2002.

An, S.-I., Kim, H., and Kim, B.-M.: Impact of freshwater discharge from the Greenland ice sheet on North Atlantic climate variability, Theoretical and Applied Climatology, 112, 29–43, https://doi.org/10.1007/s00704-012-0699-6, 2012.

Balmonte, J. P., Hasler-Sheetal, H., Glud, R. N., Andersen, T. J., Sejr, M. K., Middelboe, M., Teske, A., and Arnosti, C.: Sharp contrasts between freshwater and marine microbial enzymatic capabilities, community composition, and DOM pools in a NE Greenland fjord, Limnology and Oceanography, https://doi.org/10.1002/lno.11253, http://dx.doi.org/10.1002/lno.11253, 2019.

Bamber, J. L., Griggs, J. A., Hurkmans, R. T. W. L., Dowdeswell, J. A., Gogineni, S. P., Howat, I., Mouginot, J., Paden, J., Palmer, S., Rignot, E., and Steinhage, D.: A new bed elevation dataset for Greenland, The Cryosphere, 7, 499–510, https://doi.org/10.5194/tc-7-499-2013, 2013.

Bamber, J. L., Tedstone, A. J., King, M. D., Howat, I. M., Enderlin, E. M., van den Broeke, M. R., and Noel, B.: Land Ice Freshwater Budget of the Arctic and North Atlantic Oceans: 1. Data, Methods, and Results, Journal of Geophysical Research: Oceans, 123, 1827–1837, https://doi.org/10.1002/2017jc013605, 2018.

Beckmann, J., Perrette, M., Beyer, S., Calov, R., Willeit, M., and Ganopolski, A.: Modeling the response of Greenland outlet glaciers to global warming using a coupled flow line–plume model, The Cryosphere, 13, 2281–2301, https://doi.org/10.5194/tc-13-2281-2019, http://dx.doi.org/10.5194/tc-13-2281-2019, 2019.

Bendtsen, J., Mortensen, J., Lennert, K., and Rysgaard, S.: Heat sources for glacial ice melt in a West Greenland tidewater outlet glacier fjord: The role of subglacial freshwater discharge, Geophysical Research Letters, https://doi.org/10.1002/2015GL063846, 2015.

Catania, G., Stearns, L., Moon, T., Enderlin, E., and Jackson, R.: Future Evolution of Greenland's Marine-Terminating Outlet Glaciers, Journal of Geophysical Research: Earth Surface, https://doi.org/10.1029/2018jf004873, http://dx.doi.org/10.1029/2018JF004873, 2019.

Chu, W., Creyts, T. T., and Bell, R. E.: Rerouting of subglacial water flow between neighboring glaciers in West Greenland, Journal of Geophysical Research: Earth Surface, 121, 925–938, https://doi.org/10.1002/2015JF003705, 2016.

Citterio, M. and Ahlstrøm, A. P.: Brief communication "The aerophotogrammetric map of Greenland ice masses", The Cryosphere, 7, 445–449, https://doi.org/10.5194/tc-7-445-2013, http://dx.doi.org/10.5194/tc-7-445-2013, 2013.

Citterio, M., Sejr, M. K., Langen, P. L., Mottram, R. H., Abermann, J., Hillerup Larsen, S., Skov, K., and Lund, M.: Towards quantifying the glacial runoff signal in the freshwater input to Tyrolerfjord–Young Sound, NE Greenland, Ambio, 46, 146–159, https://doi.org/10.1007/s13280-016-0876-4, http://dx.doi.org/10.1007/s13280-016-0876-4, 2017.

Cowton, T. R., Slater, D., Sole, A., Goldberg, D., and Nienow, P.: Modeling the impact of glacial runoff on fjord circulation and submarine melt rate using a new subgrid-scale parameterization for glacial plumes, Journal of Geophysical Research: Oceans, 120, 796–812, https://doi.org/10.1002/2014JC010324, 2015.

Cowton, T. R., Todd, J. A., and Benn, D. I.: Sensitivity of tidewater glaciers to submarine melting governed by plume locations, Geophysical Research Letters, https://doi.org/10.1029/2019gl084215, http://dx.doi.org/10.1029/2019GL084215, 2019.

https://doi.org/10.5194/essd-2020-47
Preprint. Discussion started: 7 April 2020




Delhasse, A., Kittel, C., Amory, C., Hofer, S., and Fettweis, X.: Brief communication: Interest of a regional climate model against ERA5 to simulate the near-surface climate of the Greenland ice sheet, The Cryosphere Discussions, https://doi.org/10.5194/tc-2019-96, https://doi.org/10.5194/tc-2019-96, 2019.

Echelmeyer, K. and Harrison, W. D.: Jakobshavns Isbræ, West Greenland: Seasonal Variations in Velocity - or Lack Thereof, Journal of Glaciology, 36, 82–88, https://doi.org/10.3189/s0022143000005591, 1990.

Enderlin, E. M., Hamilton, G. S., Straneo, F., and Sutherland, D. A.: Iceberg meltwater fluxes dominate the freshwater budget in Greenland's iceberg-congested glacial fjords, Geophysical Research Letters, https://doi.org/10.1002/2016gl070718, 2016.

Fahnestock, M., Abdalati, W., Joughin, I. R., Brozena, J., and Gogineni, P. S.: High geothermal heat flow, basal melt, and the origin of rapid ice flow in central Greenland, Science, 294, 2338–2342, https://doi.org/10.1126/science.1065370, 2001.

Fettweis, X., Box, J. E., Agosta, C., Amory, C., Kittel, C., Lang, C., van As, D., Machguth, H., and Gallée, H.: Reconstructions of the 1900–2015 Greenland ice sheet surface mass balance using the regional climate MAR model, The Cryosphere, 11, 1015–1033, https://doi.org/10.5194/tc-11-1015-2017, http://dx.doi.org/10.5194/tc-11-1015-2017, 2017.

Fried, M., Carroll, D., Catania, G., Sutherland, D., Stearns, L., Shroyer, E., and Nash, J.: Distinct frontal ablation processes drive heterogeneous submarine terminus morphology, Geophysical Research Letters, https://doi.org/10.1029/2019gl083980, http://dx.doi.org/10.1029/2019GL083980, 2019.

Gillard, L. C., Hu, X., Myers, P. G., and Bamber, J. L.: Meltwater pathways from marine terminating glaciers of the Greenland ice sheet, Geophysical Research Letters, 43, 10,873–10,882, https://doi.org/10.1002/2016gl070969, http://dx.doi.org/10.1002/2016GL070969, 2016.

GRASS Development Team: Geographic Resources Analysis Support System (GRASS GIS) Software, Open Source Geospatial Foundation, USA, https://grass.osgeo.org, 2018.

Hawkings, J., Wadham, J., Tranter, M., Lawson, E., Sole, A., Cowton, T., Tedstone, A., Bartholomew, I., Nienow, P., Chandler, D., and et al.: The effect of warming climate on nutrient and solute export from the Greenland Ice Sheet, Geochemical Perspectives Letters, p. 94–104, https://doi.org/10.7185/geochemlet.1510, http://dx.doi.org/10.7185/geochemlet.1510, 2015.

Howat, I.: MEaSUREs Greenland Ice Mapping Project (GIMP) 2000 Image Mosaic, Version 1, https://doi.org/10.5067/4RNTRRE4JCYD, updated 2018. Used all subsets. Accessed 2020-02-04. NASA National Snow and Ice Data Center Distributed Active Archive Center, 2017a.

Howat, I.: MEaSUREs Greenland Ice Mapping Project (GIMP) Land Ice and Ocean Classification Mask, Version 1, https://doi.org/10.5067/B8X58MQBFUPA, used all subsets; Accessed 2019-03-21. NASA National Snow and Ice Data Center Distributed Active Archive Center, 2017b.

Howat, I. M., Negrete, A., and Smith, B. E.: The Greenland Ice Mapping Project (GIMP) land classification and surface elevation data sets, The Cryosphere, 8, 1509–1518, https://doi.org/10.5194/tc-8-1509-2014, http://dx.doi.org/10.5194/tc-8-1509-2014, 2014.

Hoyer, S. and Hamman, J. J.: xarray: N-D labeled Arrays and Datasets in Python, Journal of Open Research Software, 5, https://doi.org/10.5334/jors.148, http://dx.doi.org/10.5334/jors.148, 2017.

Hunter, J. D.: Matplotlib: A 2D graphics environment, Computing In Science & Engineering, 9, 90–95, 2007.

Jasiewicz, J. and Metz, M.: A new GRASS GIS toolkit for Hortonian analysis of drainage networks, Computers & Geosciences, 37, 1162–1173, https://doi.org/10.1016/j.cageo.2011.03.003, http://dx.doi.org/10.1016/j.cageo.2011.03.003, 2011.

Kamenos, N. A., Hoey, T. B., Nienow, P. W., Fallick, A. E., and Claverle, T.: Reconstructing Greenland ice sheet runoff using coralline algae, Geology, 40, 1095–1098, https://doi.org/10.1130/G33405.1, 2012.

https://doi.org/10.5194/essd-2020-47
Preprint. Discussion started: 7 April 2020




Kanna, N., Sugiyama, S., Ohashi, Y., Sakakibara, D., Fukamachi, Y., and Nomura, D.: Upwelling of Macronutrients and Dissolved Inorganic Carbon by a Subglacial Freshwater Driven Plume in Bowdoin Fjord, Northwestern Greenland, Journal of Geophysical Research: Biogeosciences, 123, 1666–1682, https://doi.org/10.1029/2017jg004248, http://dx.doi.org/10.1029/2017JG004248, 2018.

Kluyver, T., Ragan-Kelley, B., Pérez, F., Granger, B., Bussonnier, M., Frederic, J., Kelley, K., Hamrick, J., Grout, J., Corlay, S., Ivanov, P., Avila, D., Abdalla, S., and Willing, C.: Jupyter Notebooks – a publishing format for reproducible computational workflows, 2016.

Kondo, K. and Sugiyama, S.: Discharge measurement at the outlet stream of Qaanaaq Glacier in the summer 2017-2019, https://doi.org/10.22008/hokkaido/data/meltwater_discharge/qaanaaq, GEUS Data Center, 2020.

Langen, P. L., Mottram, R. H., Christensen, J. H., Boberg, F., Rodehacke, C. B., Stendel, M., van As, D., Ahlstrøm, A. P., Mortensen, J., Rysgaard, S., Petersen, D., Svendsen, K. H., Aḥalgeirsdóttir, G., and Cappelen, J.: Quantifying energy and mass fluxes controlling Godthåbsfjord freshwater input in a 5 km simulation (1991-2012), Journal of Climate, 28, 3694–3713, https://doi.org/10.1175/JCLI-D-14-00271.1, 2015.

Langley, K.: GEM river discharge measurements, https://doi.org/10.22008/asiaq/data/meltwater_discharge/gem, GEUS Data Center, 2020.

Lewis, S. M. and Smith, L. C.: Hydrologic drainage of the Greenland ice sheet, Hydrological Processes, 23, 2004–2011, https://doi.org/10.1002/hyp.7343, 2009.

Lindbäck, K., Pettersson, R., Doyle, S. H., Helanow, C., Jansson, P., Kristensen, S. S., Stenseng, L., Forsberg, R., and Hubbard, A. L.: High-resolution ice thickness and bed topography of a land-terminating section of the Greenland Ice Sheet, Earth System Science Data, 6, 331–338, https://doi.org/10.5194/essd-6-331-2014, http://dx.doi.org/10.5194/essd-6-331-2014, 2014.

Lindbäck, K., Pettersson, R., Hubbard, A. L., Doyle, S. H., van As, D., Mikkelsen, A. B., and Fitzpatrick, A. A.: Subglacial water drainage, storage, and piracy beneath the Greenland Ice Sheet, Geophysical Research Letters, https://doi.org/10.1002/2015GL065393, 2015.

Liston, G. E. and Mernild, S. H.: Greenland freshwater runoff. Part I: A runoff routing model for glaciated and nonglaciated landscapes (HydroFlow), Journal of Climate, 25, 5997–6014, https://doi.org/10.1175/JCLI-D-11-00591.1, 2012.

Livingston, S. J., Clark, C. D., Woodward, J., and Kingslake, J.: Potential subglacial lake locations and meltwater drainage pathways beneath the Antarctic and Greenland ice sheets, The Cryosphere, 7, 1721–1740, https://doi.org/10.5194/tc-7-1721-2013, 2013.

Mankoff, K. D.: Greenland liquid water runoff from 1979 through 2017, https://doi.org/10.22008/promice/data/freshwater_runoff/v01, GEUS Data Center, 2020.

Mankoff, K. D. and Tulaczyk, S. M.: The past, present, and future viscous heat dissipation available for Greenland subglacial conduit formation, The Cryosphere, 11, 303–317, https://doi.org/10.5194/tc-11-303-2017, 2017.

Mankoff, K. D., Straneo, F., Cenedese, C., Das, S. B., Richards, C. G., and Singh, H.: Structure and dynamics of a subglacial discharge plume in a Greelandic fjord, Journal of Geophysical Research: Oceans, 121, 8670–8688, https://doi.org/10.1002/2016JC011764, 2016.

Mankoff, K. D., Colgan, W., Solgaard, A., Karlsson, N. B., Ahlstrøm, A. P., van As, D., Box, J. E., Khan, S. A., Kjeldsen, K. K., Mouginot, J., and Fausto, R. S.: Greenland Ice Sheet solid ice discharge from 1986 through 2017, Earth System Science Data, 11, 769 – 786, https://doi.org/10.5194/essd-11-769-2019, https://doi.org/10.5194/essd-11-769-2019, 2019.

McKinney, W.: Data Structures for Statistical Computing in Python, in: Proceedings of the 9th Python in Science Conference, edited by van der Walt, S. and Millman, J., pp. 51 – 56, 2010.

Mernild, S., Howat, I., Ahn, Y., Liston, G., Steffen, K., Jakobsen, B., Hasholt, B., Fog, B., and van As, D.: Freshwater flux to Sermilik Fjord, SE Greenland, The Cryosphere, 4, 453–465, https://doi.org/10.5194/tc-4-453-2010, 2010.

Mernild, S. H. and Liston, G. E.: Greenland Freshwater Runoff. Part II: Distribution and Trends, 1960-2010, Journal of Climate, 25, 6015–6035, https://doi.org/10.1175/JCLI-D-11-00592.1, 2012.

https://doi.org/10.5194/essd-2020-47
Preprint. Discussion started: 7 April 2020




Mernild, S. H., Liston, G. E., Hiemstra, C. A., and Steffen, K.: Surface melt area and water balance modeling on the Greenland ice sheet 1995-2005, Journal of Hydrometeorology, 9, 1191–1211, https://doi.org/10.1175/2008JHM957.1, 2008.

Mernild, S. H., Liston, G. E., Hiemstra, C. A., Steffen, K., Hanna, E., and Christensen, J. H.: Greenland Ice Sheet surface mass-balance modelling and freshwater flux for 2007, and in a 1995–2007 perspective, Hydrological Processes, 23, 2470–2484, https://doi.org/10.1002/hyp.7354, 2009.

Mernild, S. H., Liston, G. E., van As, D., Hasholt, B., and Yde, J. C.: High-resolution ice sheet surface mass-balance and spatiotemporal runoff simulations: Kangerlussuaq, west Greenland, Arctic, Antarctic, and Alpine Research, 50, S100 008, https://doi.org/10.1080/15230430.2017.1415856, http://dx.doi.org/10.1080/15230430.2017.1415856, 2018.

Moon, T., Sutherland, D. A., Carroll, D., Felikson, D., Kehrl, L., and Straneo, F.: Subsurface iceberg melt key to Greenland fjord freshwater budget, Nature Geoscience, https://doi.org/10.1038/s41561-017-0018-z, http://dx.doi.org/10.1038/s41561-017-0018-z, 2017.

Morlighem, M., Rignot, E. J., Mouginot, J., Seroussi, H., and Larour, E.: Deeply incised submarine glacial valleys beneath the Greenland ice sheet, Nature Geoscience, 7, 418–422, https://doi.org/10.1038/NGEO2167, 2014.

Morlighem, M., Williams, C., Rignot, E., An, L., Arndt, J. E., Bamber, J., Catania, G., Chauché, N., Dowdeswell, J. A., Dorschel, B., Fenty, I., Hogan, K., Howat, I., Hubbard, A., Jakobsson, M., Jordan, T. M., Kjeldsen, K. K., Millan, R., Mayer, L., Mouginot, J., Noël, B., O'Cofaigh, C., Palmer, S. J., Rysgaard, S., Seroussi, H., Siegert, M. J., Slabon, P., Straneo, F., van den Broeke, M. R., Weinrebe, W., Wood, M., and Zinglersen, K.: IceBridge BedMachine Greenland, Version 3, https://doi.org/10.5067/2CIX82HUV88Y, used all subsets; Accessed 2018-10-28, 2017a.

Morlighem, M., Williams, C. N., Rignot, E., An, L., Arndt, J. E., Bamber, J. L., Catania, G., Chauché, N., Dowdeswell, J. A., Dorschel, B., Fenty, I., Hogan, K., Howat, I. M., Hubbard, A., Jakobsson, M., Jordan, T. M., Kjeldsen, K. K., Millan, R., Mayer, L., Mouginot, J., Noël, B. P. Y., Cofaigh, C. Ó., Palmer, S., Rysgaard, S., Seroussi, H., Siegert, M. J., Slabon, P., Straneo, F., van den Broeke, M. R., Weinrebe, W., Wood, M., and Zinglersen, K. B.: BedMachine v3: Complete bed topography and ocean bathymetry mapping of Greenland from multi-beam echo sounding combined with mass conservation, Geophysical Research Letters, https://doi.org/10.1002/2017gl074954, 2017b.

Mortensen, J., Bendtsen, J., Motyka, R. J., Lennert, K., Truffer, M., Fahnestock, M., and Rysgaard, S.: On the seasonal freshwater stratification in the proximity of fast-flowing tidewater outlet glaciers in a sub-Arctic sill fjord, Journal of Geophysical Research: Oceans, 118, 1382–1395, https://doi.org/10.1002/jgrc.20134, 2013.

Munneke, P. K., Ligtenberg, S. R. M., van den Broeke, M. R., van Angelen, J. H., and Forster, R. R.: Explaining the presence of perennial liquid water bodies in the firn of the Greenland Ice Sheet, Geophysical Research Letters, 41, 476–483, https://doi.org/10.1002/2013GL058389, 2014.

Neteler, M., Bowman, M. H., Landa, M., and Metz, M.: GRASS GIS: a multi-purpose Open Source GIS, Environmental Modelling & Software, 31, 124–130, https://doi.org/10.1016/j.envsoft.2011.11.014, 2012.

Noël, B., van de Berg, W. J., van Wessem, J. M., van Meijgaard, E., van As, D., Lenaerts, J. T. M., Lhermitte, S., Kuipers Munneke, P., Smeets, C. J. P. P., van Ulft, L. H., and et al.: Modelling the climate and surface mass balance of polar ice sheets using RACMO2 – Part 1: Greenland (1958–2016), The Cryosphere, 12, 811–831, https://doi.org/10.5194/tc-12-811-2018, http://dx.doi.org/10.5194/tc-12-811-2018, 2018.

Noël, B., van de Berg, W. J., Lhermitte, S., and van den Broeke, M. R.: Rapid ablation zone expansion amplifies north Greenland mass loss, Science Advances, 5, eaaw0123, https://doi.org/10.1126/sciadv.aaw0123, https://doi.org/10.1126/sciadv.aaw0123, 2019.

Oliphant, T. E.: A guide to NumPy, vol. 1, Trelgol Publishing USA, 2006.

https://doi.org/10.5194/essd-2020-47
Preprint. Discussion started: 7 April 2020




Perner, K., Moros, M., Otterå, O. H., Blanz, T., Schneider, R. R., and Jansen, E.: An oceanic perspective on Greenland's recent freshwater discharge since 1850, Scientific Reports, 9, https://doi.org/10.1038/s41598-019-53723-z, http://dx.doi.org/10.1038/s41598-019-53723-z, 2019.

Porter, C., Morin, P., Howat, I., Noh, M.-J., Bates, B., Peterman, K., Keesey, S., Schlenk, M., Gardiner, J., Tomko, K., Willis, M., Kelleher, C., Cloutier, M., Husby, E., Foga, S., Nakamura, H., Platson, M., Wethington, Michael, J., Williamson, C., Bauer, G., Enos, J., Arnold, G., Kramer, W., Becker, P., Doshi, A., D'Souza, C., Cummens, P., Laurier, F., and Bojesen, M.: ArcticDEM, https://doi.org/10.7910/DVN/OHHUKH, date accessed: 2019-11-14, 2018.

PROJ contributors: PROJ coordinate transformation software library, Open Source Geospatial Foundation, https://proj4.org/, 2018.

Rennermalm, A. K., Smith, L. C., Chu, V. W., Forster, R. R., Box, J. E., and Hagedorn, B.: Proglacial river stage, discharge, and temperature datasets from the Akuliarusiarsuup Kuua River northern tributary, Southwest Greenland, 2008–2011, Earth System Science Data, 4, 1–12, https://doi.org/10.5194/essd-4-1-2012, 2012.

Rennermalm, A. K., Smith, L. C., Chu, V. W., Box, J. E., Forester, R. R., van den Broeke, M. R., van As, D., and Moustafa, S. E.: Evidence of meltwater retention within the Greenland ice sheet, The Cryosphere, 7, 1433–1445, https://doi.org/10.5194/tc-7-1433-2013, 2013.

Schulte, E., Davison, D., Dye, T., and Dominik, C.: A multi-language computing environment for literate programming and reproducible research, Journal of Statistical Software, 46, 1–24, 2012.

Seabold, S. and Perktold, J.: Statsmodels: Econometric and statistical modeling with python, in: 9th Python in Science Conference, 2010.

Shreve, R. L.: Movement of water in glaciers, Journal of Glaciology, 11, 205–214, 1972.

Slater, D. A., Straneo, F., Felikson, D., Little, C. M., Goelzer, H., Fettweis, X., and Holte, J.: Estimating Greenland tidewater glacier retreat driven by submarine melting, The Cryosphere, 13, 2489–2509, https://doi.org/10.5194/tc-13-2489-2019, http://dx.doi.org/10.5194/tc-13-2489-2019, 2019.

Smith, L. C., Chu, V. W., Yang, K., Gleason, C. J., Pitcher, L. H., Rennermalm, A. K., Legleiter, C. J., Behar, A. E., Overstreet, B. T., Moustafa, S. E., Tedesco, M., Forster, R. R., LeWinter, A. L., Finnegan, D. C., Sheng, Y., and Balog, J.: Efficient meltwater drainage through supraglacial streams and rivers on the southwest Greenland ice sheet, Proceedings of the National Academy of Sciences, 112, 1001–1006, https://doi.org/10.1073/pnas.1413024112, 2015.

Stallman, R. M.: EMACS the extensible, customizable self-documenting display editor, Proceedings of the ACM SIGPLAN SIGOA symposium on Text manipulation -, https://doi.org/10.1145/800209.806466, 1981.

Stevens, L. A., Straneo, F., Das, S. B., Plueddemann, A. J., Kukulya, A. L., and Morlighem, M.: Linking glacially modified waters to catchment-scale subglacial discharge using autonomous underwater vehicle observations, The Cryosphere, 10, 417–432, https://doi.org/10.5194/tc-10-417-2016, 2016.

Stevens, L. A., Hewitt, I. J., Das, S. B., and Behn, M. D.: Relationship Between Greenland Ice Sheet Surface Speed and Modeled Effective Pressure, Journal of Geophysical Research: Earth Surface, 123, 2258–2278, https://doi.org/10.1029/2017jf004581, http://dx.doi.org/10.1029/2017JF004581, 2018.

Straneo, F., Curry, R. G., Sutherland, D. A., Hamilton, G. S., Cenedese, C., Våge, K., and Stearns, L. A.: Impact of fjord dynamics and glacial runoff on the circulation near Helheim Glacier, Nature Geoscience, 4, 322–327, https://doi.org/10.1038/NGEO1109, 2011.

Sugiyama, S., Sakakibara, D., Matsuno, S., Yamaguchi, S., Matoba, S., and Aoki, T.: Initial field observations on Qaanaaq ice cap, northwestern Greenland, Annals of Glaciology, 55, 25–33, https://doi.org/10.3189/2014aog66a102, http://dx.doi.org/10.3189/2014AoG66A102, 2014.

https://doi.org/10.5194/essd-2020-47
Preprint. Discussion started: 7 April 2020




Tange, O.: GNU Parallel - The Command-Line Power Tool, ;login: The USENIX Magazine, 36, 42–47, https://doi.org/10.5281/zenodo.16303, http://www.gnu.org/s/parallel, 2011.

Tedstone, A., Bartholomew, I., Chandler, D., Cowton, C., Mair, D., Sole, A., Wadham, J., , and Nienow, P.: Proglacial discharge measurements, Leverett Glacier, south-west Greenland (2009-2012), https://doi.org/10.5285/17c400f1-ed6d-4d5a-a51f-aad9ee61ce3d, accessed 2020-02-21, 2017.

Trusel, L. D., Das, S. B., Osman, M. B., Evans, M. J., Smith, B. E., Fettweis, X., McConnell, J. R., Noël, B. P. Y., and van den Broeke, M. R.: Nonlinear rise in Greenland runoff in response to post-industrial Arctic warming, Nature, 564, 104–108, https://doi.org/10.1038/s41586-018-0752-4, http://dx.doi.org/10.1038/s41586-018-0752-4, 2018.

Tsutaki, S., Sugiyama, S., Sakakibara, D., Aoki, T., and Niwano, M.: Surface mass balance, ice velocity and near-surface ice temperature on Qaanaaq Ice Cap, northwestern Greenland, from 2012 to 2016, Annals of Glaciology, 58, 181–192, https://doi.org/10.1017/aog.2017.7, http://dx.doi.org/10.1017/aog.2017.7, 2017.

van As, D., Bech Mikkelsen, A., Holtegaard Nielsen, M., Box, J. E., Claesson Liljedahl, L., Lindbäck, K., Pitcher, L., and Hasholt, B.: Hypsometric amplification and routing moderation of Greenland ice sheet meltwater release, The Cryosphere, 11, 1371–1386, https://doi.org/10.5194/tc-11-1371-2017, http://dx.doi.org/10.5194/tc-11-1371-2017, 2017.

van As, D., Hasholt, B., Ahlstrøm, A. P., Box, J. E., Cappelen, J., Colgan, W., Fausto, R. S., Mernild, S. H., Mikkelsen, A. B., Noël, B. P. Y., Petersen, D., and van den Broeke, M. R.: Reconstructing Greenland Ice Sheet meltwater discharge through the Watson River (1949–2017), Arctic, Antarctic, and Alpine Research, https://doi.org/10.1080/15230430.2018.1433799, 2018.

Van Rossum, G. and Drake Jr, F. L.: Python reference manual, Centrum voor Wiskunde en Informatica Amsterdam, 1995.

Vandecrux, B., MacFerrin, M., Machguth, H., Colgan, W. T., van As, D., Heilig, A., Stevens, C. M., Charalampidis, C., Fausto, R. S., Morris, E. M., and et al.: Firn data compilation reveals widespread decrease of firn air content in western Greenland, The Cryosphere, 13, 845–859, https://doi.org/10.5194/tc-13-845-2019, http://dx.doi.org/10.5194/tc-13-845-2019, 2019.

Werder, M. A., Hewitt, I. J., Schoof, C. G., and Flowers, G. E.: Modeling channelized and distributed subglacial drainage in two dimensions, Journal of Geophysical Research, 118, 2140–2158, https://doi.org/10.1002/jgrf.20146, 2013.

Yang, K., Smith, L. C., Fettweis, X., Gleason, C. J., Lu, Y., and Li, M.: Surface meltwater runoff on the Greenland ice sheet estimated from remotely sensed supraglacial lake infilling rate, Remote Sensing of Environment, 234, 111 459, https://doi.org/10.1016/j.rse.2019.111459, http://dx.doi.org/10.1016/j.rse.2019.111459, 2019.

Zeh, H.: The Physical Basis of The Direction of Time, The Frontiers Collection, Springer Berlin Heidelberg, 2007.

Zuo, Z. and Oerlemans, J.: Modelling albedo and specific balance of the Greenland ice sheet: calculations for the Søndre Strømfjord transect, Journal of Glaciology, 42, 305–317, https://doi.org/10.3189/s0022143000004160, http://dx.doi.org/10.3189/S0022143000004160, 1996.

https://doi.org/10.5194/essd-2020-47
Preprint. Discussion started: 7 April 2020


Open Access Earth System Science Data Discussions

## Figures

### Overview

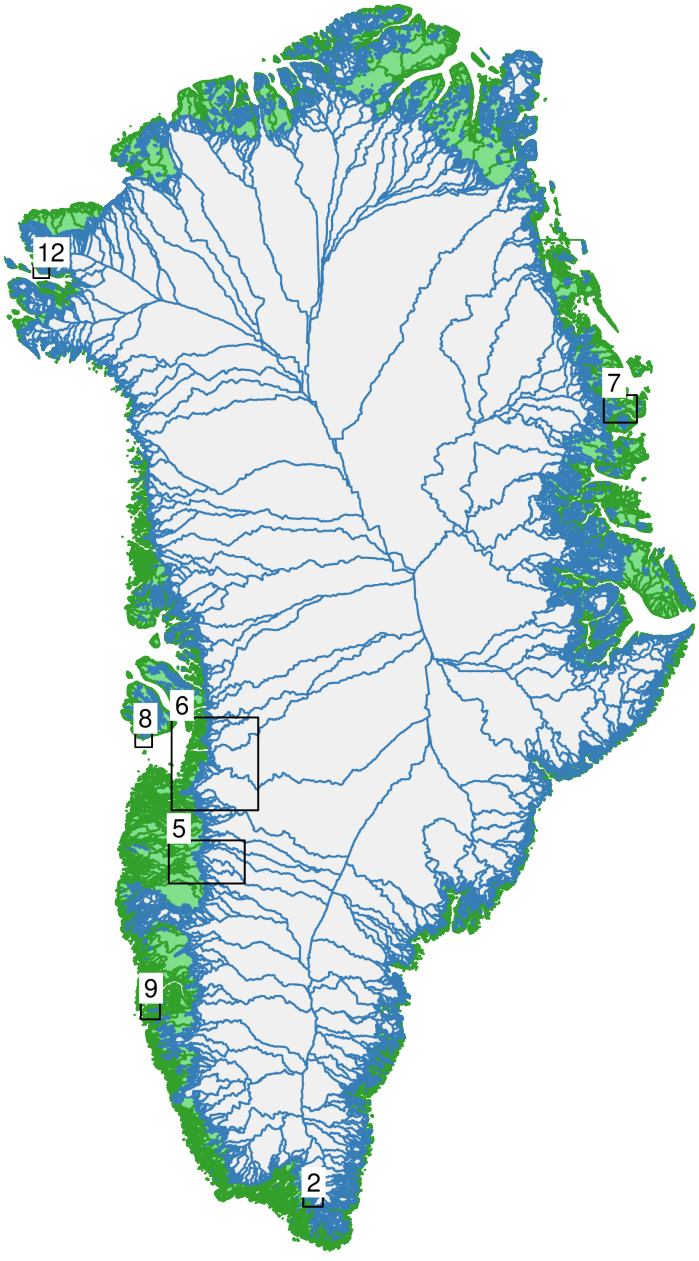


**Figure 1.** Overview showing ice basins (blue) and land basins (green), and insets of all other figures.

https://doi.org/10.5194/essd-2020-47
Preprint. Discussion started: 7 April 2020


Open Access Earth System Science Data Discussions

**Coverage**

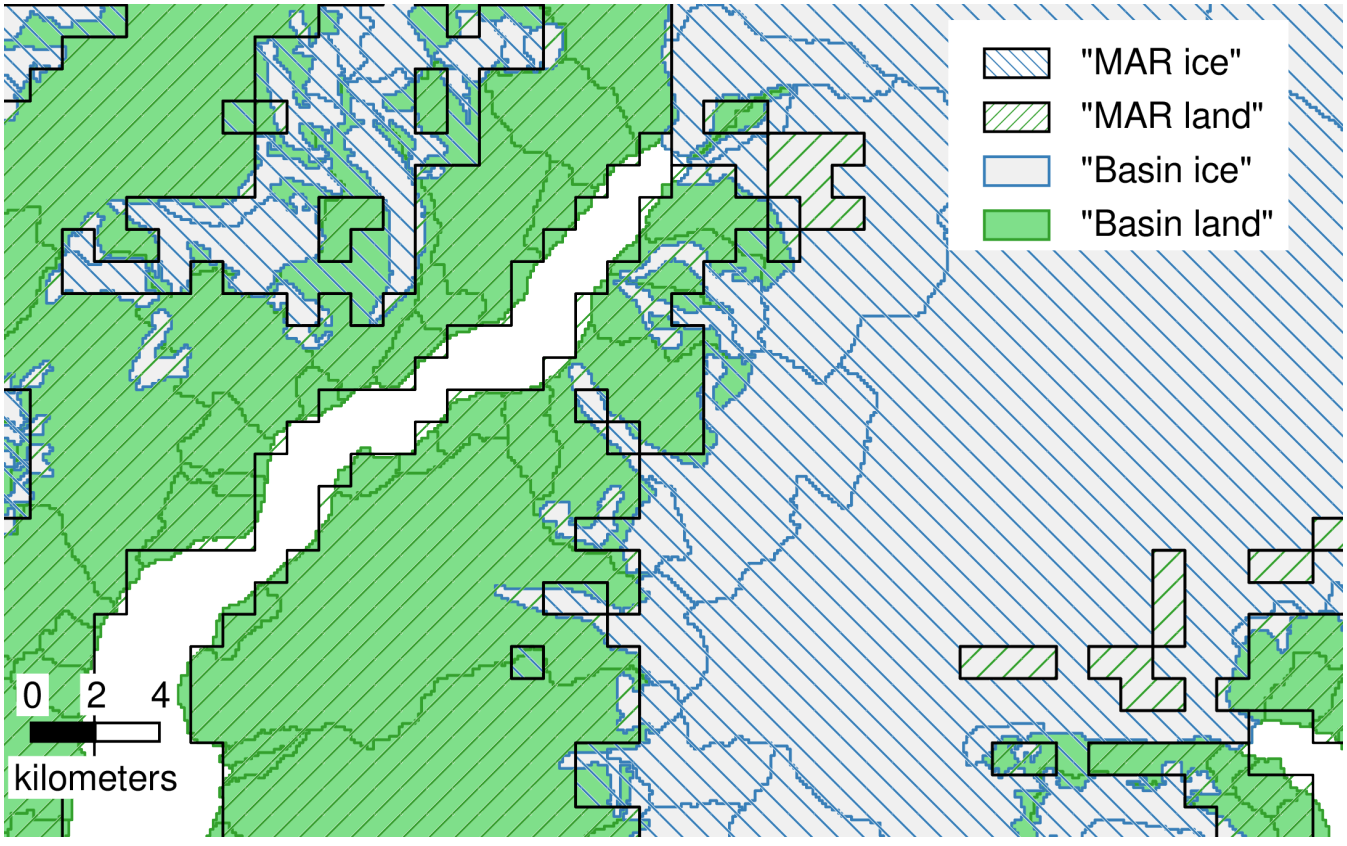


**Figure 2.** Example of model (MAR) and basin misalignment (MAR ice over basin land, or MAR land over basin ice). See Sec. 3.1.

https://doi.org/10.5194/essd-2020-47
Preprint. Discussion started: 7 April 2020


Open Access Earth System Science Data Discussions

**Annual Runoff**

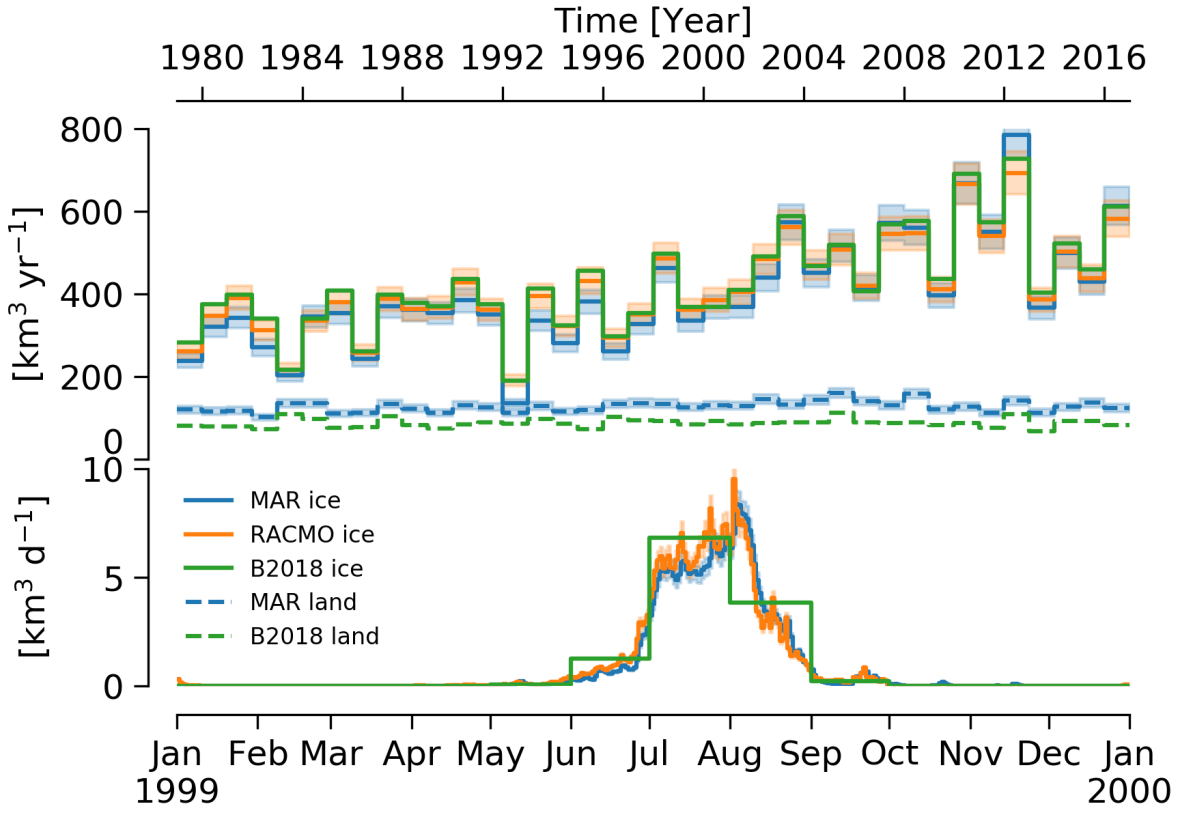


**Figure 3.** Top panel: Annual Greenland ice sheet runoff from RACMO and MAR as calculated in this product, and B2018 (Bamber et al., 2018). Dashed lines show runoff from land. Bottom panel: 1999 ice runoff at daily resolution (this) or monthly for B2018.

https://doi.org/10.5194/essd-2020-47
Preprint. Discussion started: 7 April 2020


Open Access Earth System Science Data Discussions

**Watson runoff**

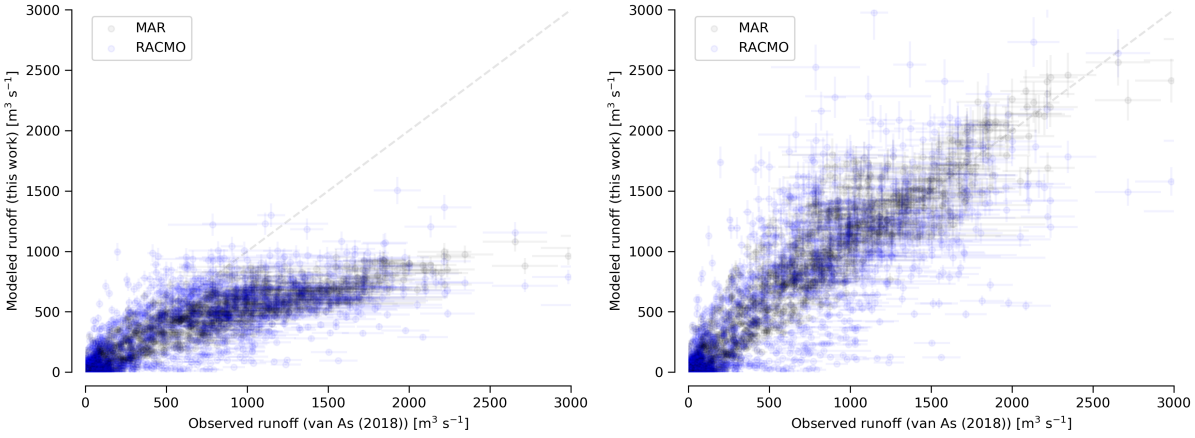


**Figure 4.** Comparison for Watson River basin runoff between van As et al. (2018) and this product (this product based on ArcticDEM basin in Fig. 5). Left panel is runoff from the Watson River basin as defined by ArcticDEM. Right panel is runoff from the Watson River basin plus the two large basins immediately to the south. MAR includes both ice and land contribution to the outlet while RACMO only includes ice contribution.

https://doi.org/10.5194/essd-2020-47
Preprint. Discussion started: 7 April 2020


Open Access Earth System Science Data Discussions

**Watson basins**

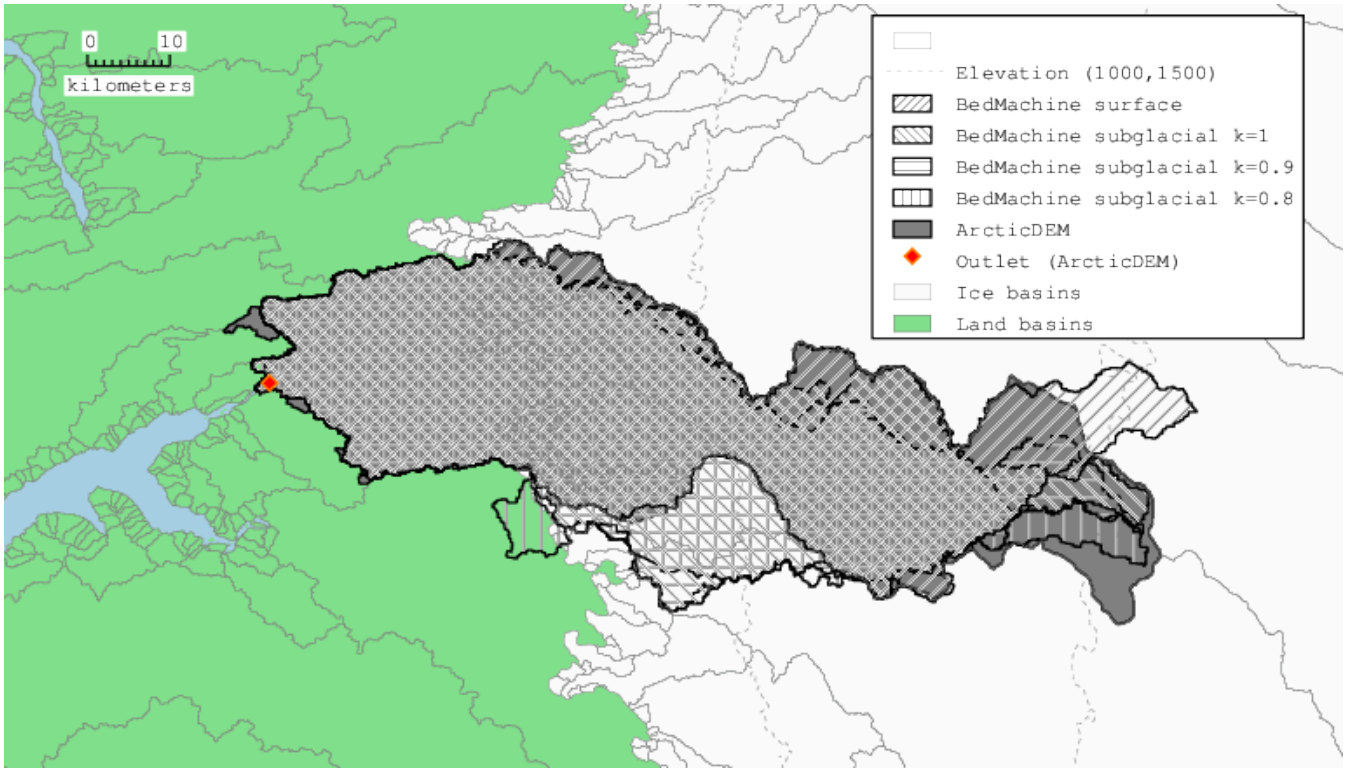


**Figure 5.** Watson basins based on different routing assumptions. ArcticDEM basin used for "this work" in Fig. 4.

https://doi.org/10.5194/essd-2020-47
Preprint. Discussion started: 7 April 2020


Open Access Earth System Science Data Discussions

**Change in Outlet**

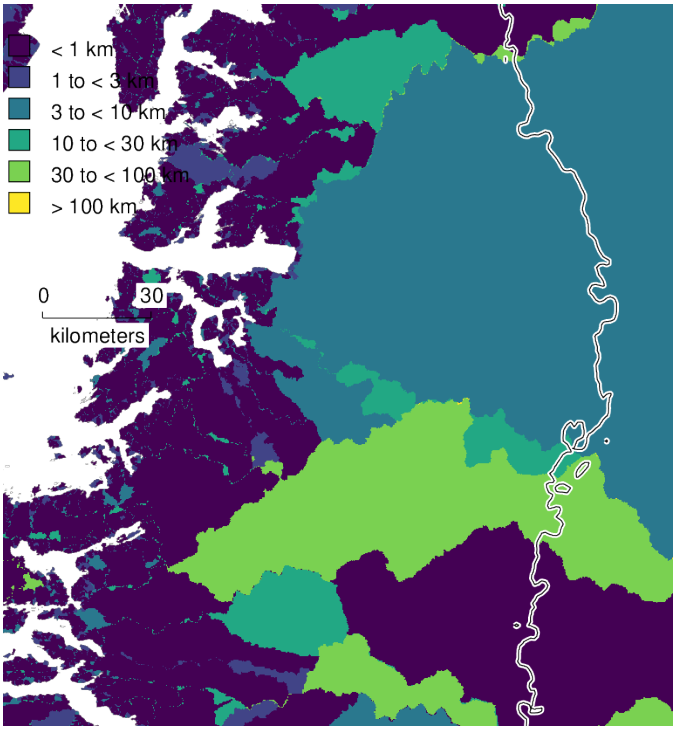


**Figure 6.** Change in outlet location between baseline ArcticDEM surface routing and BedMachine v3 surface routing is shown for every grid cell. Region is zoomed in near Sermeq Kujalleq (Jakobshavn Isbræ). White-and-black contour line shows 2000 m elevation, above which little runoff occurs.

https://doi.org/10.5194/essd-2020-47
Preprint. Discussion started: 7 April 2020


Open Access Earth System Science Data Discussions

**GEM Basin**

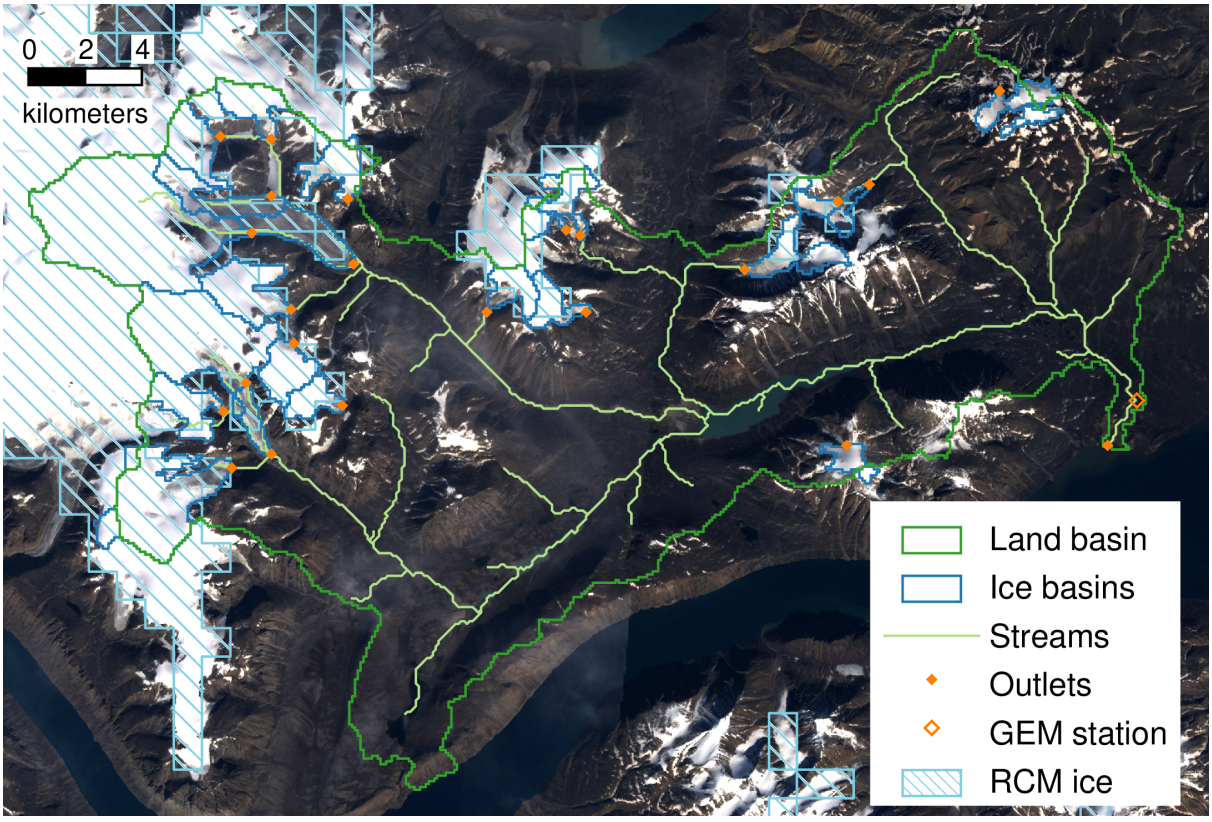


**Figure 7.** Zackenberg basin for GEM outlet. Note two small glaciers without correstponding MAR or RACMO ice cells. See Fig. 10 for comparisons between GEM and MAR discharge at this location. Also visible is basin artifact at southern-most portion of basin. Because basins < 1 $km^2$ are absorbed into their largest neighbor, here small basins clearly outside the basin (south of the coastal mountain range) are absorbed into the basin. Basemap from Howat et al. (2014); Howat (2017a).

https://doi.org/10.5194/essd-2020-47
Preprint. Discussion started: 7 April 2020


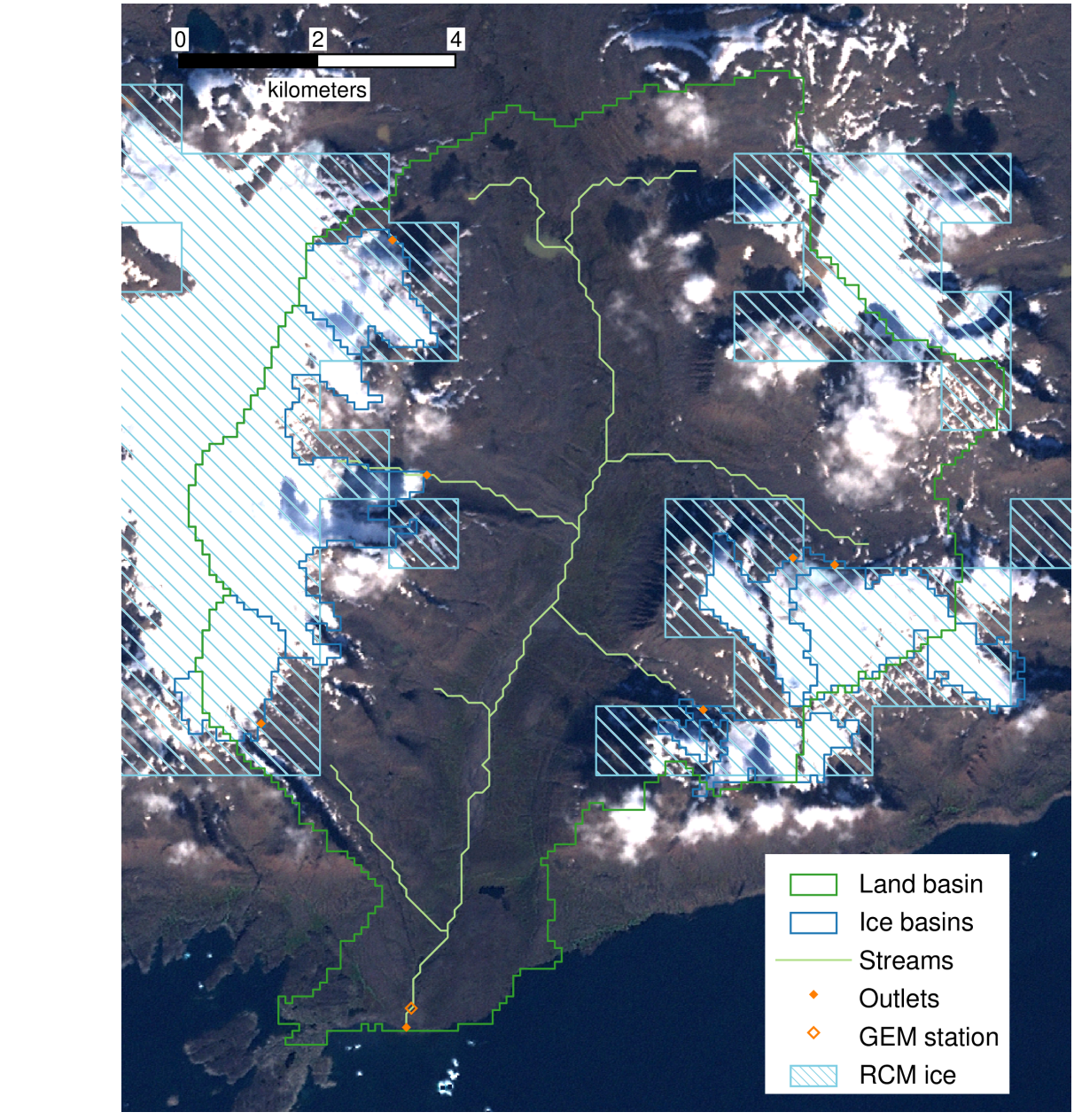


**Figure 8.** Røde Elv basin for GEM outlet. See figures 10 and 11 for comparisons between GEM and MAR discharge at this location. Basemap from Howat et al. (2014); Howat (2017a).

https://doi.org/10.5194/essd-2020-47
Preprint. Discussion started: 7 April 2020


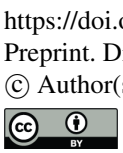

Open Access Earth System Science Data Discussions

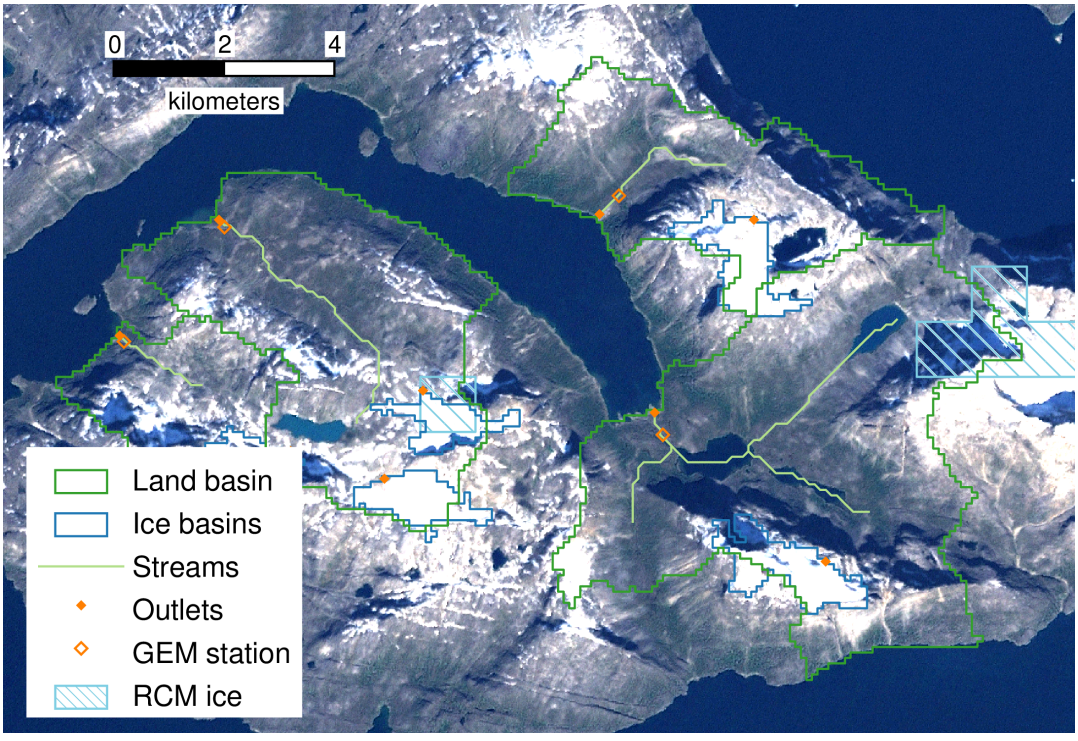


**Figure 9.** GEM basins for Kingigtorssuaq, Kobbefjord, Oriartorfik, and Teqinngalip outlets. Note that except for one RCM ice cell, no ice basins have RCM runoff estimates. Furthermore, at the eastern edge of the image RCM ice cells exist where no ice basin exists (that RCM runoff is discarded). See figures 10 and 11 for comparisons between GEM and MAR discharge at these location. Basemap from Howat et al. (2014); Howat (2017a).

https://doi.org/10.5194/essd-2020-47
Preprint. Discussion started: 7 April 2020


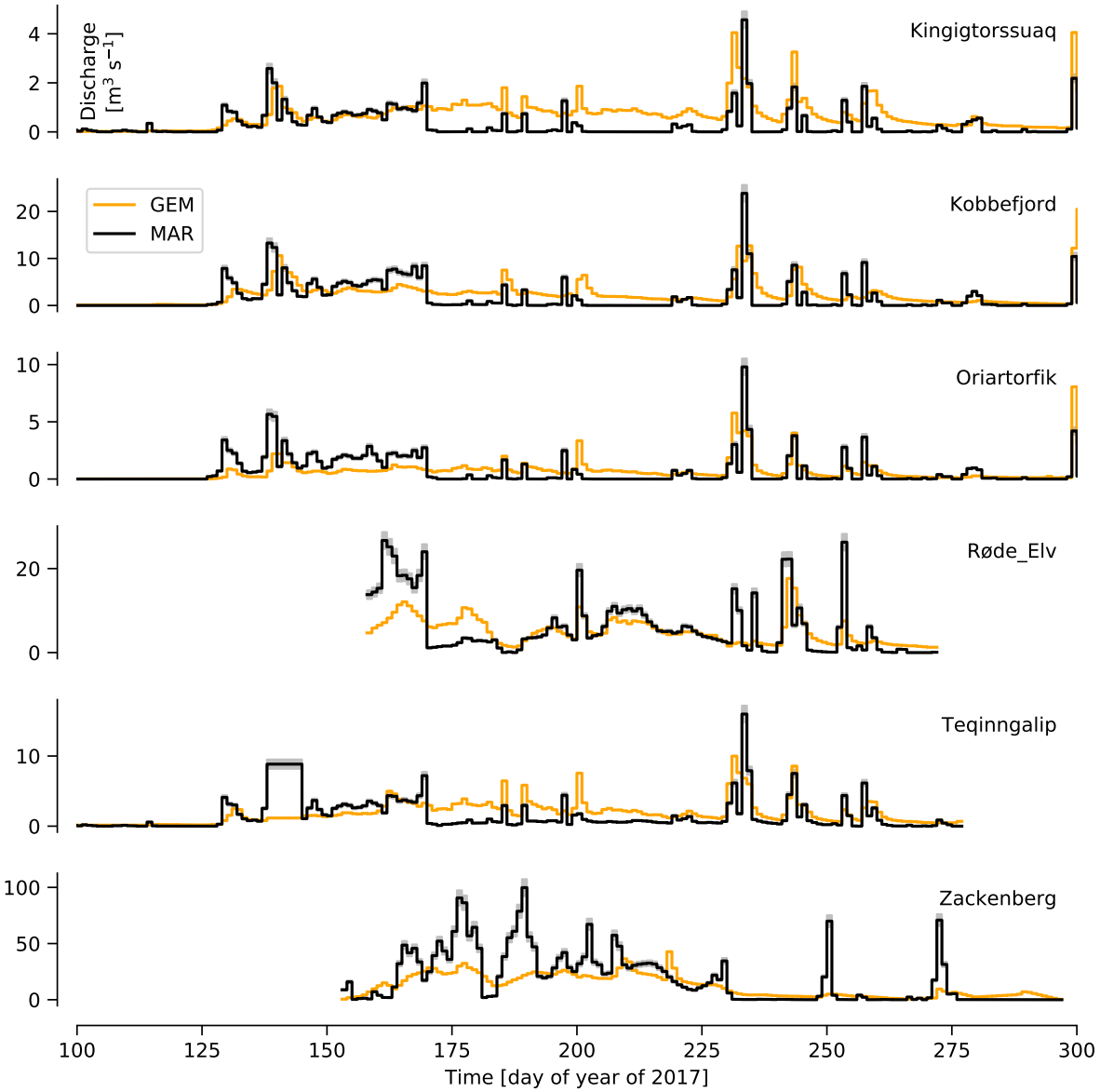


**Figure 10.** Time series of GEM observed MAR ice and land runoff for basins shown in Figures 7, 8, and 9. Only 2017 shown because that is the only year where data exists at Røde Elv.

https://doi.org/10.5194/essd-2020-47
Preprint. Discussion started: 7 April 2020


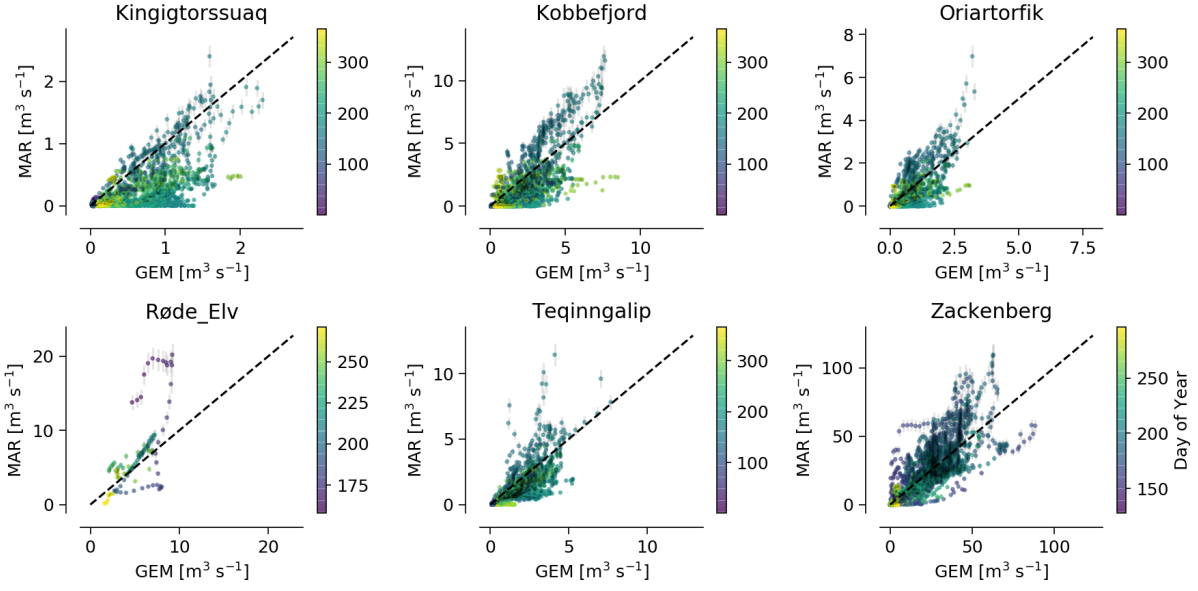


**Figure 11.** Scatter plot of 10-day averages of GEM and MAR runoff for basins shown in Figures 7, 8, and 9. Data for all available years at all stations are shown.

https://doi.org/10.5194/essd-2020-47
Preprint. Discussion started: 7 April 2020


Open Access Earth System Science Data Discussions

**Qaanaaq**

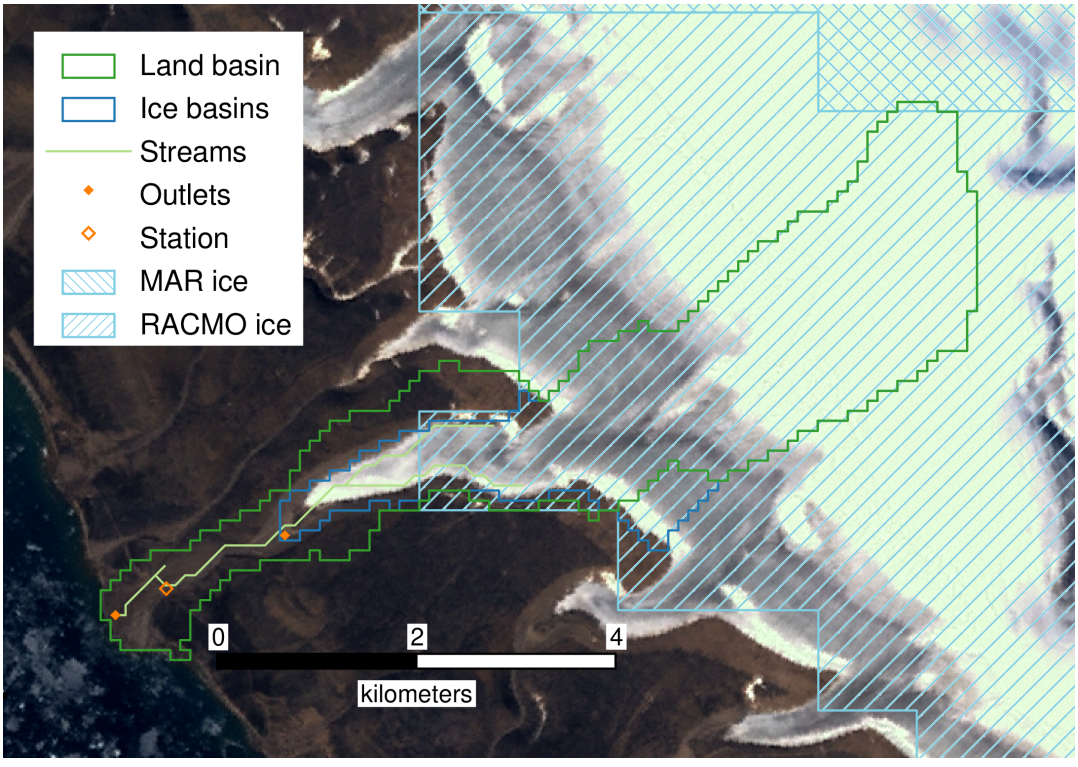


**Figure 12.** Plan view of Qaanaaq basin. Note that MAR ice cells only cover ~1 % of ice basin, while RACMO ice cells cover ~90 % of ice basin. See Figure 13 for runoff data from this basin. Basemap from Howat et al. (2014); Howat (2017a).

https://doi.org/10.5194/essd-2020-47
Preprint. Discussion started: 7 April 2020


Open Access Earth System Science Data Discussions

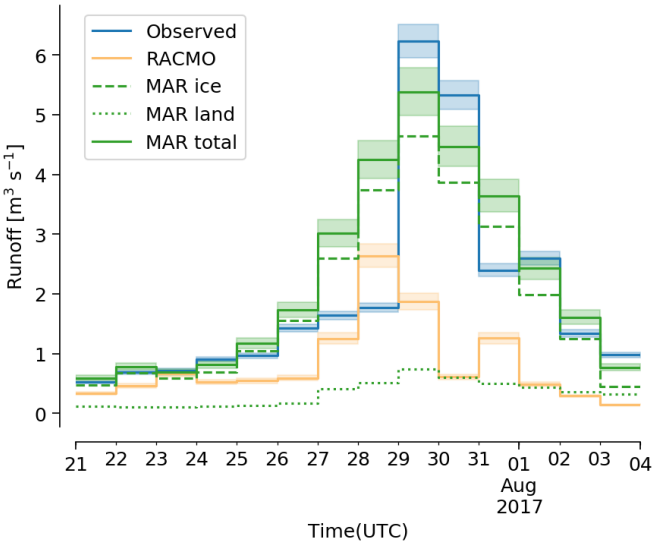


**Figure 13.** Time series of observed and modeled runoff at Qaanaaq basin outlet (see Figure 12). Displayed uncertainty is 9 % for observations and 15 % for RCMs. Uncertainty only shown for total MAR runoff, not ice or land components.

https://doi.org/10.5194/essd-2020-47
Preprint. Discussion started: 7 April 2020


Open Access Earth System Science Data Discussions

**Leverett Glacier**

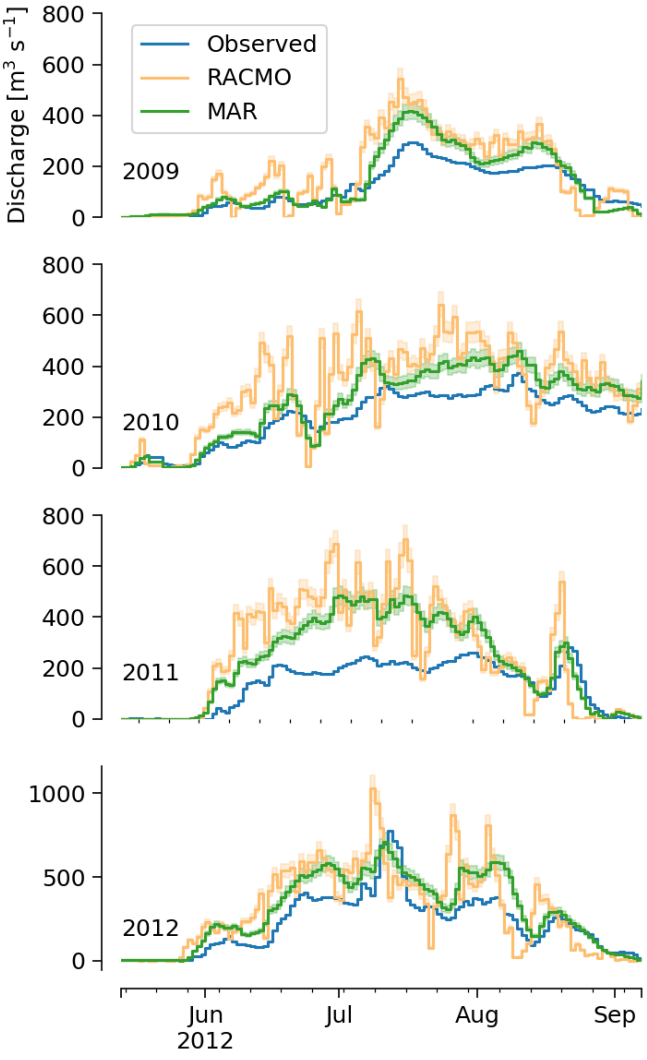


**Figure 14.** Time series of Leverett glacier observed discharge vs. this product.

https://doi.org/10.5194/essd-2020-47
Preprint. Discussion started: 7 April 2020


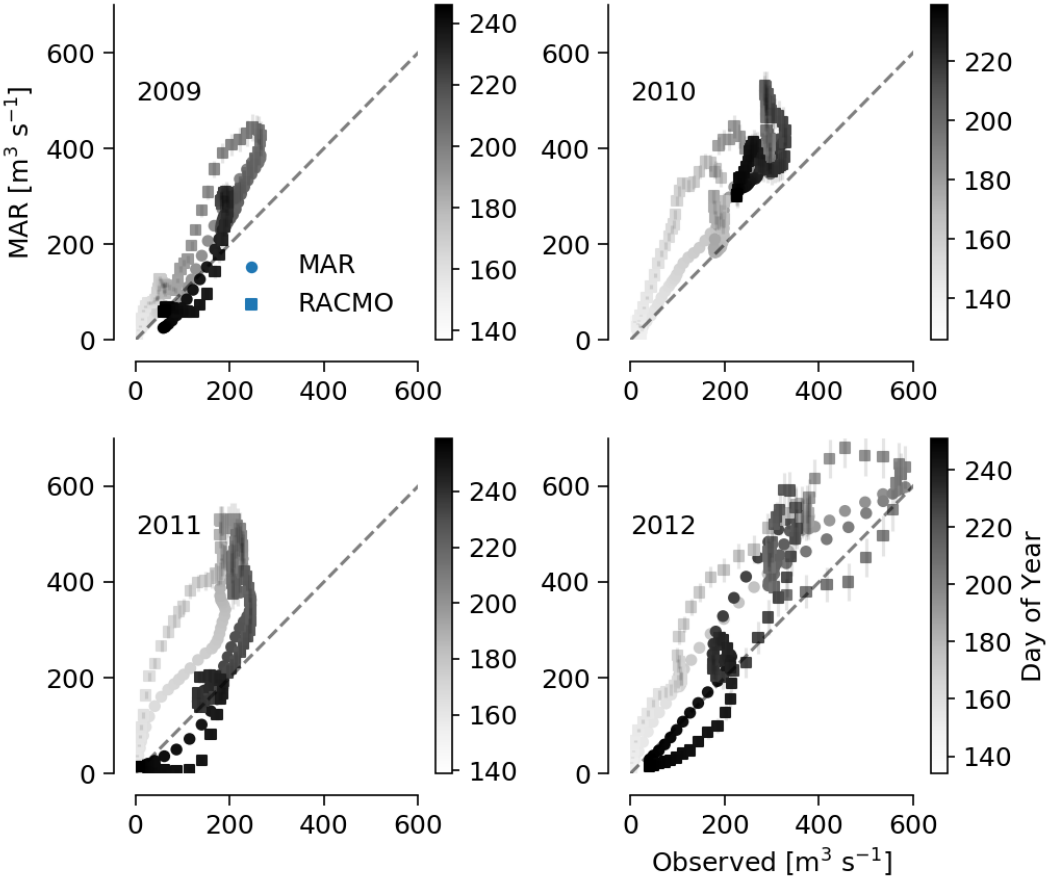


**Figure 15.** Scatter plot of Leverett glacier observed discharge vs. this product.

https://doi.org/10.5194/essd-2020-47
Preprint. Discussion started: 7 April 2020



## Appendix A: Software

This work was performed using only open-source software, primarily `GRASS GIS` (Neteler et al., 2012) and `Python` (Van Rossum and Drake Jr, 1995), in particular the `Jupyter` (Kluyver et al., 2016), `pandas` (McKinney, 2010), `numpy` (Oliphant, 2006), `statsmodel` (Seabold and Perktold, 2010), `x-array` (Hoyer and Hamman, 2017), and `Matplotlib` (Hunter, 2007) packages. The entire work was performed in `Emacs` (Stallman, 1981) using `Org Mode` (Schulte et al., 2012). The `parallel` (Tange, 2011) tool was used to speed up processing. We used `proj4` (PROJ contributors, 2018) to compute the errors in the EPSG 3413 projection. All code used in this work is available in the Supplemental Online Material.

https://doi.org/10.5194/essd-2020-47
Preprint. Discussion started: 7 April 2020


Open Access Earth System Science Data Discussions

**Appendix B: Changing basins with changing routing schemes**

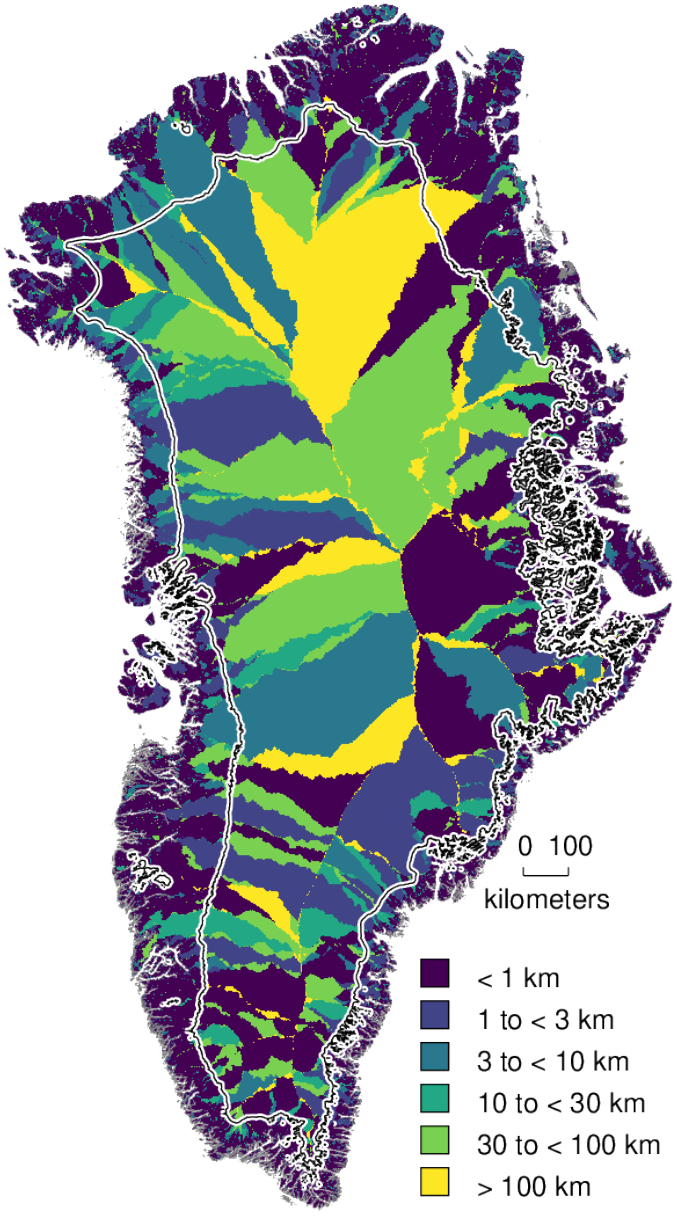


**Figure B1.** Same as Fig. 6 but for all of Greenland not zoomed in.

https://doi.org/10.5194/essd-2020-47
Preprint. Discussion started: 7 April 2020


Open Access Earth System Science Data Discussions

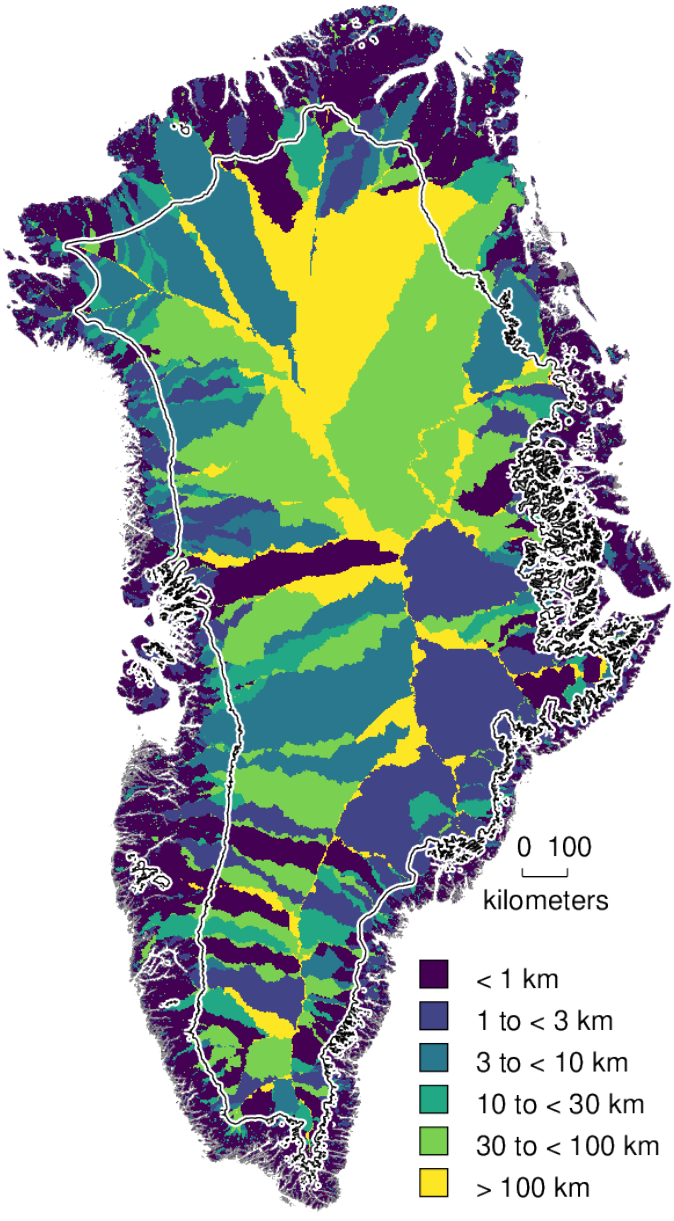


**Figure B2.** Same as Fig. B1, but comparing BedMachine surface with Bedmachine 100 % subglacial pressure.

https://doi.org/10.5194/essd-2020-47
Preprint. Discussion started: 7 April 2020


Open Access Earth System Science Data Discussions

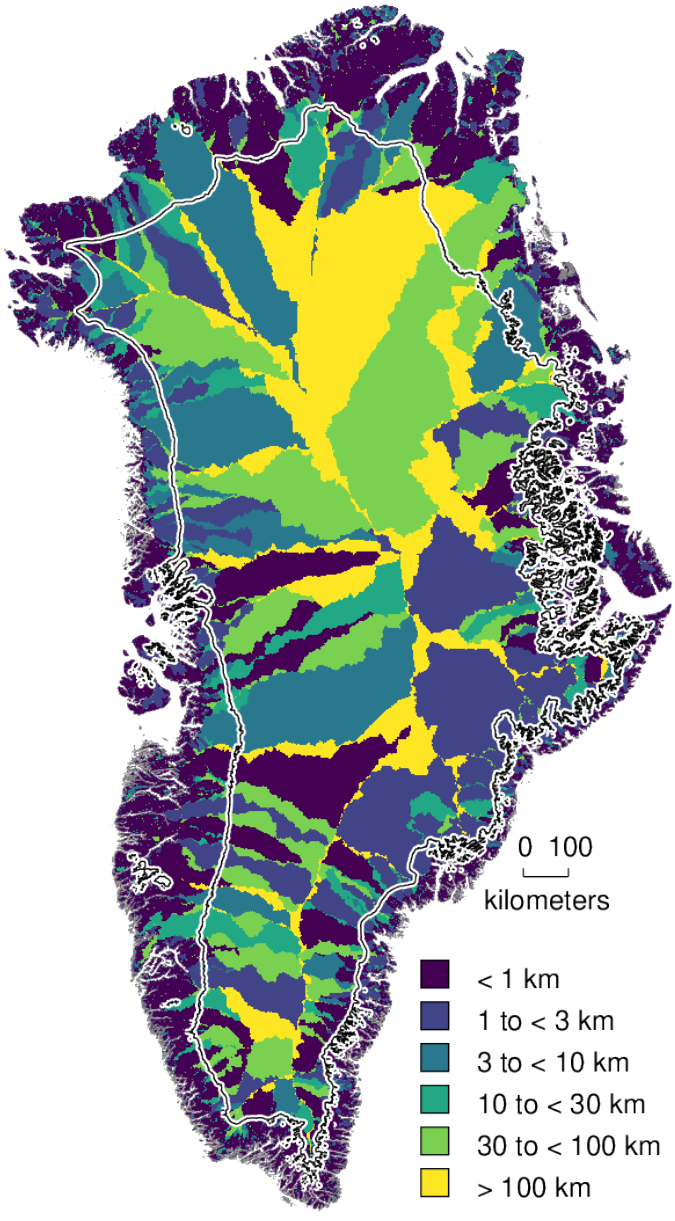


**Figure B3.** Same as Fig. B1, but with 90 % subglacial pressure.

https://doi.org/10.5194/essd-2020-47
Preprint. Discussion started: 7 April 2020


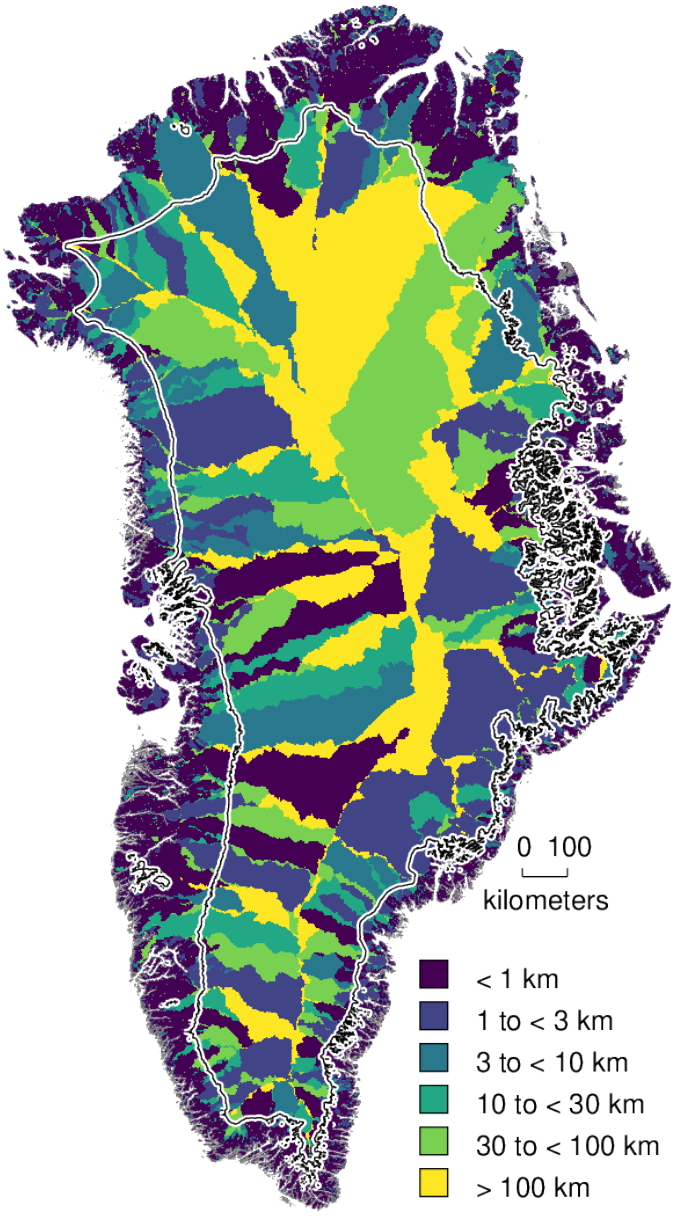


**Figure B4.** Same as Fig. B1, but with 80 % subglacial pressure.

https://doi.org/10.5194/essd-2020-47
Preprint. Discussion started: 7 April 2020


Open Access Earth System Science Data Discussions

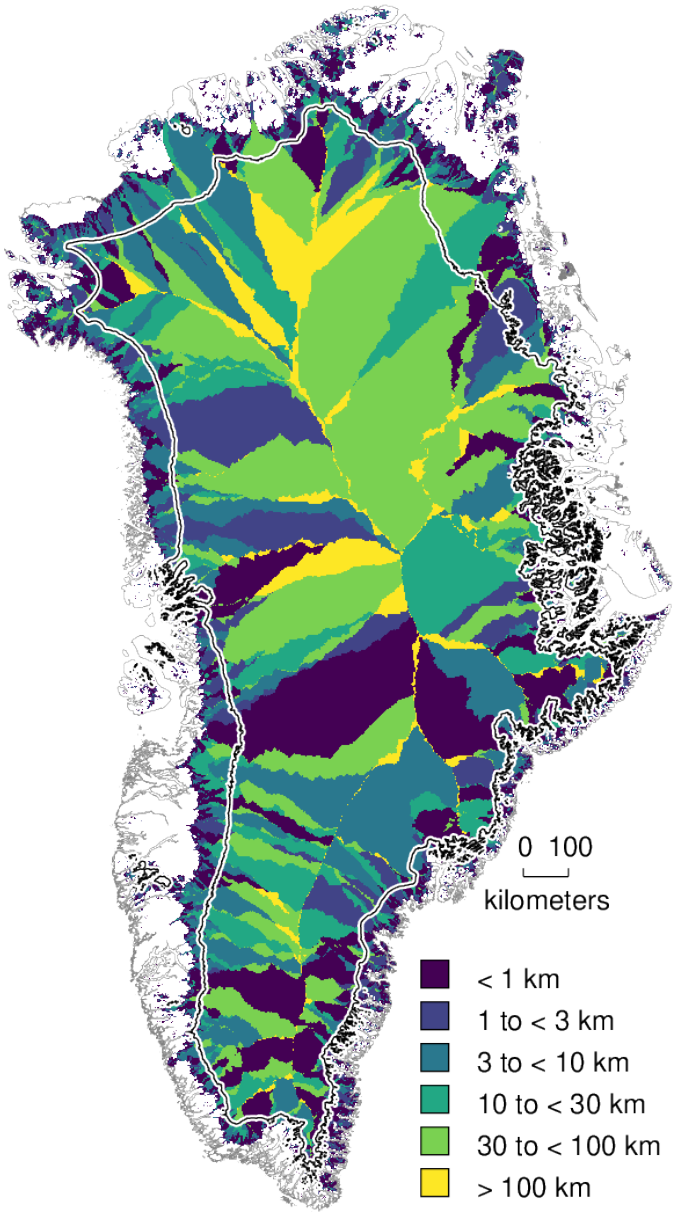


**Figure B5.** Same as Fig. B1 but comparing ice margin outlet change, not coastal outlet change.

https://doi.org/10.5194/essd-2020-47
Preprint. Discussion started: 7 April 2020


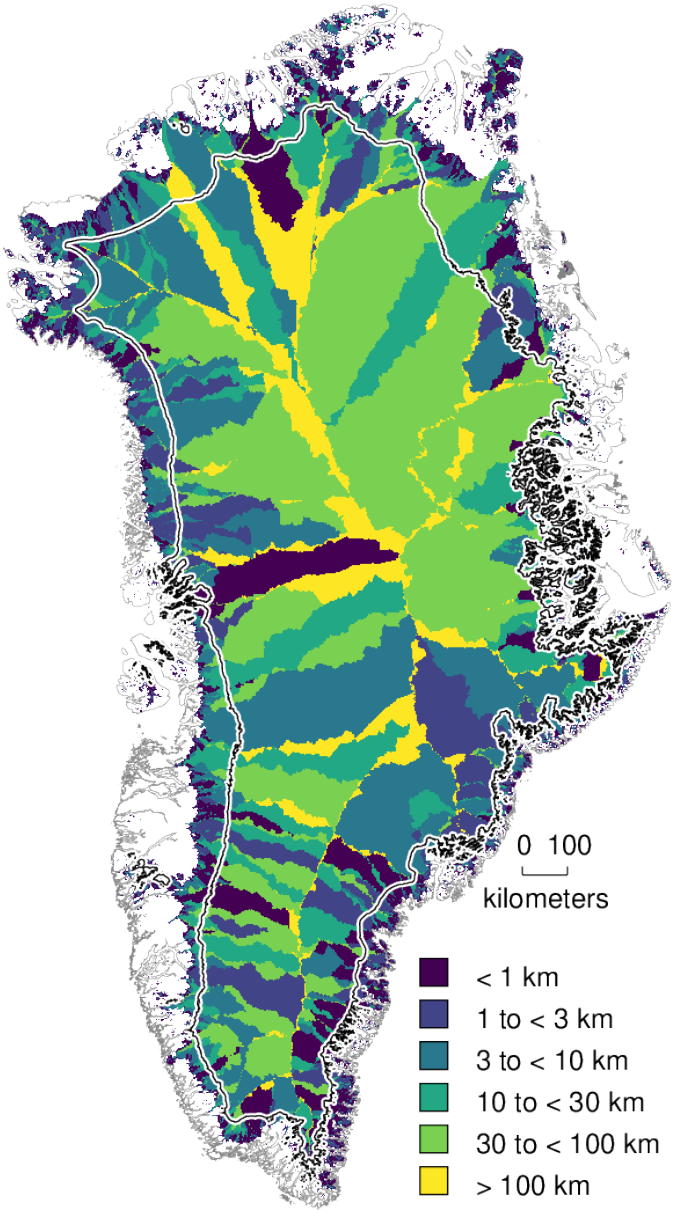


**Figure B6.** Same as Fig. B2, but ice margin outlet rather than coastal outlet. Same as Fig B5 but comparing BedMachine surface with BedMachine 100 % subglacial pressure.

https://doi.org/10.5194/essd-2020-47
Preprint. Discussion started: 7 April 2020


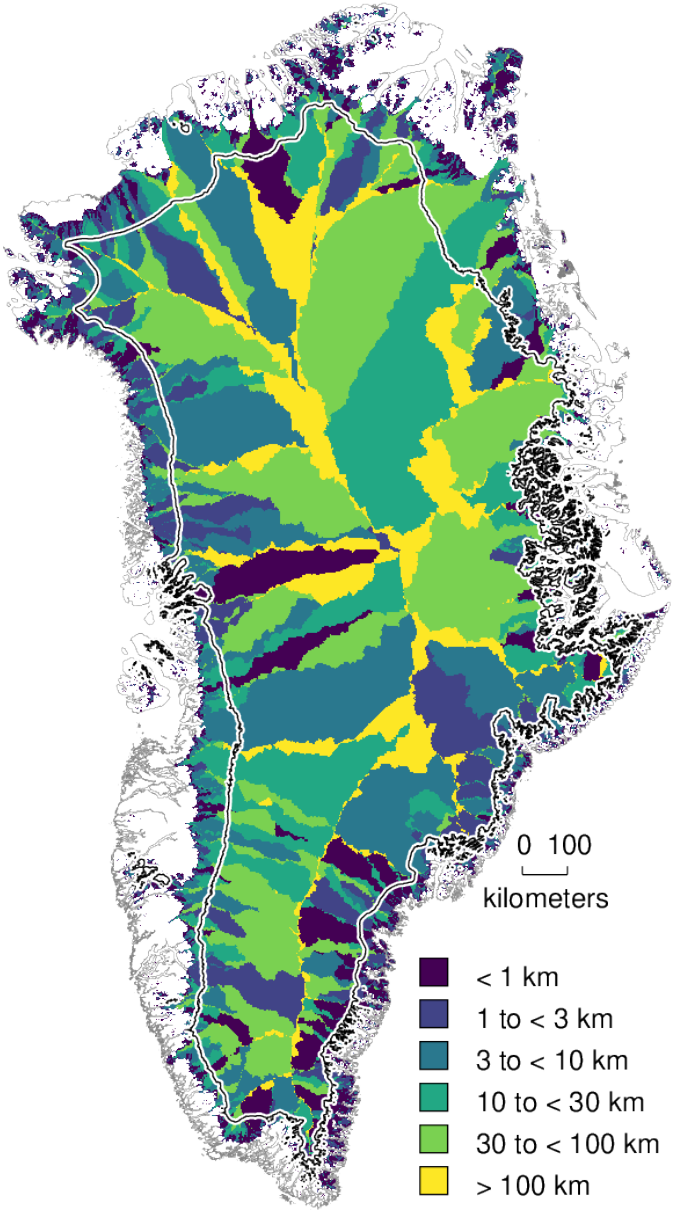


**Figure B7.** Same as Fig. B3, but ice margin outlet rather than coastal outlet. Same as Fig B5 but with 90 % subglacial pressure.

https://doi.org/10.5194/essd-2020-47
Preprint. Discussion started: 7 April 2020


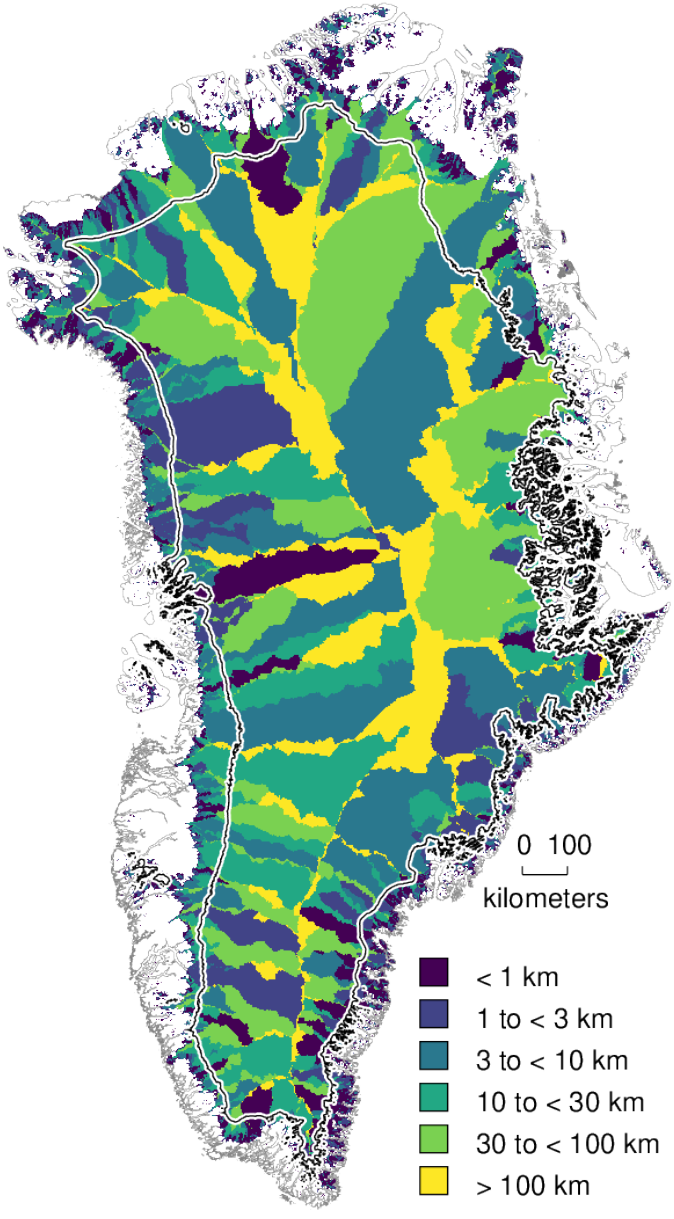


**Figure B8.** Same as Fig. B4, but ice margin outlet rather than coastal outlet. Same as Fig B5 but with 80 % subglacial pressure.